체육학 석사학위 논문

# Computational Frameworks for Determination of Muscle-Modes during Multi-Directional Postural Sway

**2018년 08월**


서울대학교 대학원

체육교육과

**Prabhat Pathak**

# Computational Frameworks for Determination of Muscle-Modes during Multi-Directional Postural Sway

지도교수 박 재 범

이 논문을 체육학 석사학위논문으로 제출함

**2018년 04월**

서울대학교 대학원

체육교육과

**Prabhat Pathak**

**Prabhat Pathak**의 석사학위논문을 인준함

**2018년 05월**

위 원 장 ..... (인)

부위원장 ..... (인)

위 원 ..... (인)

## Abstract

# Computational Frameworks for Determination of Muscle-Modes during Multi-Directional Postural Sway

**Prabhat Pathak**

**Department of Physical Education**

**The Graduate School**

**Seoul National University**

The purpose of the study was to evaluate various computational frameworks for determination of muscle-modes (M-modes) namely PCA and NMF. PCA imposes orthogonal constraint whereas, NMF imposes non-negativity constraint. This allows for various interpretation of the physiological nature of the M-modes extracted using these two computational frameworks. Based on that, we utilized a multi-directional postural sway task to determine the differences between the M-modes. Hence, we can postulate that the degrees of freedom (DOF) was decreased using both computational frameworks and DOF extracted using NMF was higher than PCA. Further, on average synergy index for all direction were hypothesized to be greater than 0.

8 healthy young adults were recruited for the study. The task included using ankle strategy to slowly moving one's center of pressure (COP) to about 80% of maximal voluntary deviation in four directions: anterior, posterior, medial (left) and lateral (right). 15 trials in total was performed for each direction. 11 muscles located at the lower limb and trunk were recorded from the right side of the body. The data was divided into two phases: Quasi-static and Dynamic phases. The integrated EMG (IEMG) value for all trails for all directions were stacked to calculate the M-modes for both analysis and separately for the two phases. Further, M-modes extracted using PCA was utilized to calculate synergy index for each direction and both phases separately.

It was determined that the COP in anterior direction was significantly higher than rest of the directions ($p < 0.05$). Joint angles were found to be have deviation higher around the ankle than rest of the joints for all directions. The DOF of M-modes extracted using NMF was determined to be $5.25 \pm 1.04$ and $5.25 \pm 0.46$ for quasi-static and dynamic phases respectively. However, The DOFs for M-modes extracted using NMF was determined to be 3 for both phases. An independent t-test revealed that DOF of M-modes extracted using NMF was significantly higher than PCA for both phases ($p < 0.05$). For both NMF and PCA analysis, the muscle grouping were determined to have certain directional dominance. Further, similarity index extracted using NMF and PCA revealed that M-modes were similar across subjects for both phases. Finally, average synergy index across subjects for both phases was found to be greater than 0 with no significant differences between directions.

The results supported all of our hypothesis with DOF for NMF being higher than PCA and synergy index being greater than 0 for all directions. Further, we attempted to distinguish the differences between the M-modes extracted using NMF and PCA while trying to relate them to behavior of neural activity at different levels of neuro-motor hierarchy (cortical and sub-cortical). The non-negativity constraint imposed by NMF allows for components of M-modes to be positive which aligns well with the activation behavior of muscles. Further, the basis vectors extracted using NMF had a higher probability of overlap similar to neural behavior at the cortical level. In case of PCA, the orthogonal constraint allows for both positive and negative values for M-modes which shows deviation of muscle activation from a certain baseline. Further, the basis vectors had a lower

probability of overlap similar to the neural behavior and also the synergy index extracted using PCA are known to have subcortical origin. Hence, the M-modes extracted using PCA might show neural behavior at the subcortical level. However, in order to confirm the neuro-motor hierarchy of M-modes extracted using NMF and PCA a clinical study might be required.

**Keywords:** Muscle modes (M-modes), Principal component analysis (PCA), Non-negative matrix factorization (NMF), Multi-directional sway, Degrees of freedom (DOF), Synergy, Neuro-motor hierarchy

**Student Number:** 2016-23105

# Table of Contents

# List of Figures

# List of Tables

# I. Introduction

## 1. Problem statement

The premise of the thesis lies on evaluation of computational frameworks involved in determination of the muscle coordination during certain postural control. For such a task, there are numerous muscles acting together to stabilize center of pressure (COP) in various directions. Human body with large number of muscles has a large degrees of freedom. Henceforth, the human neuromotor system is deemed to be redundant which requires the central controller to choose a specific solution to a problem with infinitely many solutions (Latash, Scholz, & Schöner, 2007). This issue was first addressed by Bernstein as problem of motor redundancy (Nikolai Bernstein, 1966). There has been numerous studies addressing the issue of postural control and understanding the mechanism behind control of posture to ultimately reduce the redundancy associated with it. Different variables are taken into account to understand the human postural control system which ranges from kinematic (e.g. COM, joint angles)(Oba, Sasagawa, Yamamoto, & Nakazawa, 2015), kinetic (e.g. force, COP) (Ferdjallah, Harris, Smith, & Wertsch, 2002) to physiological (e.g. muscles) (Woollacott, Shumway-Cook, & Nashner, 1986). In order to coordinate these numerous elements (muscles), it has been postulated that the controller aims towards grouping these elements (muscles) depending on the functional nature of the task (Krishnamoorthy, Latash, Scholz, & Zatsiorsky, 2003; Latash, Scholz, & Schöner, 2002). Originating from the cortical level, the neural signals controlling these muscles are organized into groups or modules called distributed processing modules (DPMs) (J. C. Houk, 2005). Two loops were found to be present in the brain structures to control these neural signals with first loop including cerebellum and cortex & second including basal ganglia and cortex (J. C. Houk, 2005). In a descending pathway, the neural signals are converged through each of these levels with decrease in degrees of freedom to relate the neuronal signals to the physical variables (J. C. Houk, 2005). Hence, these groups or modules of muscles in our case are known as muscle modes (M-modes).

These M-modes can be determined using various computational frameworks. Few of them includes Few of these include principal component analysis (PCA) (Krishnamoorthy et al., 2003), non-negative matrix factorization (NMF) (d'Avella & Tresch, 2002), independent component analysis (ICA) (Kutch, Kuo, Bloch, & Rymer, 2008) and singular value decomposition (SVD) (Sabatini, 2002). There has been numerous studies attempting towards comparing the compatibility of these methods in determining the M-modes (Tresch, Cheung, & d'Avella, 2006). Based on numerous criteria such as original basis vectors, subspace spanned by basis vectors, original activation coefficients and similarity with neurophysiological behaviour of the muscles during the task, NMF and PCA were found to perform the best (Tresch et al., 2006). Further, these two computational methods has been widely used as the core of M-mode determination in the field of motor control from understanding the basic nature of grouping of muscles during certain task (Roh, Rymer, Perreault, Yoo, & Beer, 2013) to an indicator of neuromuscular impairment (Bizzi & Cheung, 2013; Cheung et al., 2012). However, proponents of each of these methods constantly argue about viability of using the methods for determination of M-modes. In case of NMF, the muscle activations are constrained to be positive with modes prescribing a subspace within the positive quadrant. This is argued to be similar to physiological nature of muscle activation (Danion & Latash, 2011; Roh et al., 2013). While for PCA, orthogonal constraints are imposed on the modes passing through the mean of the data cloud which is utilized to compute the deviation of the muscle activation from a certain baseline (Danion & Latash, 2011; Latash, 2012). This is tethered towards understanding the functional nature of the task. Further, the functional nature and constraint imposed by PCA also allowed us to determine if these modes are coordinated together to maintain stable value of COP. This coordination of modes to perform certain task is formulated through concept of synergy (NA Bernstein, 1947; Nikolai Bernstein, 1966; Latash, 2008). In layman's term 'synergy' can be simply understood as 'working together'. The quantification of synergy is done through the framework of uncontrolled manifold analysis (UCM) and index of synergy is calculated (Latash, 2008; Scholz & Schöner, 1999).

Depending on the constraint provided by these computational frameworks, the variability accounted for by NMF is more likely to be shared among the modes so probability of activation of a

single muscle in more than a single mode is high. For PCA, the orthogonal constraint imposes the probability of modes to not share their variability is lower so, likelihood of a single muscle to activate on more than one mode is low as well. This behaviour has been commonly observed in postural sway task due to the directional dependence of muscle activation (Danion & Latash, 2011; Latash, 2012). Based on this number of modes extracted using NMF is likely to be higher than PCA for the same task. This has been observed in a study comparing NMF and PCA to general muscle and joint modes for various upper extremity task. Even though, there was not a significant difference, the modes extracted from NMF was relatively higher for both types of modes (Lambert-Shirzad & Van der Loos, 2016). Hence, we formulated following hypothesis based on the nature of these computational frameworks.

*Hypothesis – I*: Mode control (reduced degree of freedom) is observed in two ***computational methods (PCA, NMF)***.

*Hypothesis – II*: Number of modes extracted using ***NMF is larger*** than using PCA.

*Hypothesis – II*: A ***synergistic co-ordination of muscle modes*** exists in multi-directional postural sway (Synergy Index > 0).

Finally, based on the computational frameworks and nature of the modes, we will try to put forward the notion of hierarchy of M-modes extracted using these two computational frameworks.

# II. Background and Literature Review

## 1. Anatomy of lower extremity

The lower extremity contains large portion of the muscles in a human body since it is responsible for bearing the weight of the body during bipedal locomotion and maintain upright posture. Hence, the lower extremity muscles are denser and larger in order to maintain stability of the body. The objective of our study is understanding of postural control during multi-directional postural sway so a brief understanding of the anatomy of the muscles involved during postural control especially during movement in different direction would be insightful.

In studies related to postural control, human body has been frequently modelled as an inverted pendulum (Gage, Winter, Frank, & Adkin, 2004; Kuo, 2007) which is converting multi-joint system into a single-joint system. This system even though quite simple is quite difficult to equilibrate even without any external forces acting on it. Hence, a fine control in interaction between muscles and joints are required to maintain balance within the system. Therefore, our primary focus on this anatomical understanding of the lower extremity would be to reveal the functions of muscles in movement of joints in lower extremity specifically, hip, knee and ankle. Also in order to understand the movement of these joints, muscles involved in the movement of the segments generating the movement at the joints is also necessary. We will also only be concentrating on the eccentric muscles as the goal is to understand the motion from the normalized posture to a certain direction. This would give a clearer picture of muscles involved in the voluntary motion of muscles in specified direction using ankle strategy.

**Table 1:** Muscle function table denoting the lowering extremity muscles involved in anterior-posterior and medio-lateral movement(Bowden & Bowden, 2014; Palastanga et al., 2006) .

| | | Anterior-Posterior Directional Movement | | Medial-Lateral Directional Movement | |
|---|---|---|---|---|---|
| | | **Extension/Plantarflexion** | **Flexion/Dorsiflexion** | **Adduction/ Inversion** | **Abduction/ Eversion** |
| **JOINTS** | **HIP** | 1. Gluteus Maximus<br>2. Semitendinosus<br>3. Semimembranosus<br>4. Biceps Femoris | 1. Paoas Major<br>2. Iliacus<br>3. Pectineus<br>4. Rectus Femoris<br>5. Sartorius | 1. Adductor Magnus<br>2. Adductor Longus<br>3. Adductor Brevis<br>4. Gracilis<br>5. Pectineus | 1. Gluteus Maximus<br>2. Gluteus Medius<br>3. Gluteus Minimus<br>4. Tensor Fascia Lata |
| | **KNEE** | 1. Rectus Femoris<br>2. Vastus Lateralis<br>3. Vastus Medialis<br>4. Vastus Intermedius<br>5. Tensor Fascia Lata | 1. Semitendinosus<br>2. Semimembranosus<br>3. Biceps Femoris<br>4. Gastrocnemius<br>5. Gracilis<br>6. Sartorius | ***Lateral Flexion**<br>1. Quadratus lumborum<br>2. Intertransversarii<br>3. External Oblique<br>4. Internal Oblique<br>5. Rectus Abdominis<br>6. Erector Spinae<br>7. Multifidus | ***Lateral Flexion**<br>1. Quadratus lumborum<br>2. Intertransversarii<br>3. External Oblique<br>4. Internal Oblique<br>5. Rectus Abdominis<br>6. Erector Spinae<br>7. Multifidus |
| | **ANKLE** | 1. Gastrocnemius<br>2. Soleus | 1. Tibialis Anterior<br>2. Extensor Digitorum Longus<br>3. Extensor Hallucis Longus<br>4. Perneus Tertius | 1. Tibialis Posterior<br>2. Tibialis Anterior | 1. Peroneus Longus<br>2. Peroneus Brevis<br>3. Peroneus Tertius |
| **SEGMENTS** | **TRUNK** | 1. Quadratus Lumborum<br>2. Multifidus<br>3. Semispinalis<br>4. Erector Spinae<br>5. Interspinales | 1. Rectus Abdominis<br>2. External Oblique<br>3. Internal Oblique<br>4. Psoas Minor<br>5. Psoas Major | | |
| | **THIGH** | 1. Biceps Femoris<br>2. Semitendinosus<br>3. Semimembranosus<br>4. Adductor Magnus | 1. Psoas Major<br>2. Iliacus<br>3. Tensor Fasciae Latae<br>4. Sartorius<br>5. Rectus Femoris<br>6. Pectineus | 1. Gluteus Maximus<br>2. Gracilis<br>3. Adductor Longus<br>4. Adductor Brevis<br>5. Adductor Magnus | 1. Piriformis<br>2. Gluteus Maximus<br>3. Tensor Fasciae Latae<br>4. Sartorius |
| | **SHANK** | 1. Rectus Femoris<br>2. Vastus Lateralis<br>3. Vastus Medialis<br>4. Vastus Intermedius<br>5. Gracilis | 1. Sartorius<br>2. Biceps Femoris<br>3. Semitendinosus<br>4. Semimembranosus<br>5. Gastrocnemius<br>6. Plantaris<br>7. Popliteus | | |
| | **FOOT** | 1. Gastrocnemius<br>2. Soleus<br>3. Plantaris<br>4. Felxor Hallucis Longus<br>5. Felxor Digitorium Longus<br>6. Tibialis Posterior<br>7. Peroneus Longus<br>8. Peroneus Brevis | 1. Tibialis Anterior<br>2. Extensor Hallucis Longus<br>3. Extensor Digitorum Longus<br>4. Peroneus Tertius | 1. Tibialis Anterior<br>2. Extensor Hallucis Longus<br>3. Flexor Hallucis Longus<br>4. Flexor Digitorium Longus | 1. Extensor Digitorum Longus<br>2. Peroneus Tertius<br>3. Peroneus Longus<br>4. Peroneus Brevis |

**The above table is concentrated on explaining the eccentric movement from a normal stance to the specified four position. Color code has been given for the associated movement. Anterior – Blue, Posterior – Orange, Medial – Green and Lateral – Yellow*

### *1.1. Muscles involved in anterior-posterior (AP) directional movement*

The AP directional movement is associated with the movement of different joints and body segment in lower extremity and trunk in the sagittal plane.

Referring to table-1, from proximal to distal direction, it can be seen that the AP directional movement of the hip are controlled by the two group of muscles, hip extensors and flexors. The hip

extensors includes the hamstring muscles and gluteus maximus which has thick fibers that runs down and attaches itself to the femur. These muscles are primarily located at the dorsal part of upper leg. These muscles functioning to extend the hip become activated during the anterior movement of the body as they work together to extend the hip joint to counter the moment induced at the hip joint and maintain and upright posture. In case of the flexors, the muscles are primarily on the frontal part of the upper leg and work together and relatively activated during the posterior movement of the body to maintain an upright position. When we look at the segments associated with the AP movement of the hip joint, trunk and thigh are the segments working together. During anterior movement, trunk and thigh needs to be extended. In case of the trunk extension, the muscles are primarily located at the dorsal part of the trunk and the muscles working towards thigh extension are the muscles situated on the dorsal part of the upper leg similar to that of the hip joint extensors. Whereas for the posterior movement, trunk and thigh needs to be flexed. For trunk flexion, the muscles located at the frontal part of the trunk are relatively active and in case of thigh flexion, the muscles working together to achieve that is similar to the hip joint flexors.

When we look at the knee joint, the AP directional movement is facilitated by the knee extensors and flexors. The anterior directional movement requires the knee to be flexed in order to maintain an upright posture. The flexion of the knee is facilitated by the muscles located at the dorsal part of the upper and lower leg. The muscles involved for upper legs are similar to that of hip extensors while the lower leg includes Gastrocnemius. The knee joint flexion is combined with extension of thigh and flexion of shank. The muscles involved in extension of thigh has already been discussed above whereas, for shank flexion, the muscles are located primarily on the dorsal part of the upper leg similar to that of knee flexors. In case of the posterior directional movement of the body, the knee needs to be extended which is generally performed by the muscles located at the frontal part of the upper leg. The associated thigh flexion and shank extension follows knee extension. The shank extensors are the muscles located primarily at the frontal part of the upper leg which are similar to that of the knee extensors.

Finally, moving on to the ankle joint, the muscles primarily concerned with the movement in the anterior direction are the muscles facilitating ankle joint plantar flexion. These muscles include the muscles situated at the dorsal part of the lower leg mainly Gastrocnemius and Soleus. The plantar flexion of the ankle joint is combined with the shank flexion (mentioned above) and foot plantar flexion. The foot plantar flexors includes muscles involved in ankle joint plantar flexion and muscles running down to the foot digits. In case of the posterior movement of the body, the ankle joint is dorsiflexed. These dorsiflexors include the muscles situated at the front part of the lower leg and the muscles running down to the foot digits. The dorsiflexion of the ankle is combined with the shank extension (mentioned above) and foot dorsiflexion. The dorsiflexors of the foot are the same as the dorsiflexors of the ankle joint.

### *1.2. Muscles involved in medio-lateral (ML) directional movement*

The ML directional movement is associated with the movement of different joints and body segment in lower extremity and trunk in the frontal plane.

Again referring to table-1, from proximal to distal direction, it can be seen that the ML directional movement of the hip are controlled by the two group of muscles, hip adductors and abductors. For medial directional movement, hip is required to be adducted to counter the moment induced at the hip joint. The hip adductors include the muscles located at the medial part of the upper leg. Even though, there are two segments trunk and thigh associated with the movement of the hip, the trunk movement can be considered to be independent from the hip movement. Then, the remaining thigh adductor muscles is similar to that as the hip adductors with the inclusion of Gluteus maximus. In case of the lateral movement, abduction is required to counter the lateral directional hip moment. The hip abductors include the muscles concentrated on the lateral portion of the upper leg especially around the Gluteus maximus. The abduction of the hip is associated with the abduction of the thigh and the muscles involved in this movement includes the muscles in similar area as that of the hip abductors.

When we look at the knee joint, the medio-lateral directional movement when moving using ankle strategy does not fall within the degrees of freedom of the knee. The segment shank is also shares the similar mechanism as the knee joint. Hence, the medio-lateral movement of knee is associated with the only thigh (mentioned above).

Finally, moving onto the ankle joint, for medial directional movement, ankle joint is required to be inverted to counter the moment induced at the ankle. These ankle inverters include Tibialis posterior and anterior. The ankle inverters are combined with the foot inverters which includes the Tibialis anterior and the muscles running down to the foot digits from the shank. In case of the lateral directional movement, ankle joint is required to be everted. These ankle everters include the muscles located at the lateral pat of the foot which are similar to that of the associated foot eversion.

# 2. Modular control of multi-muscles and its computational frameworks

## *2.1. Non-negative matrix factorization (NMF)*

Non-negative matrix factorization (NMF) is another factor analysis technique implemented in dimension reduction (Lee & Seung, 1999, 2001). The premise behind this method is that if we are to be given a non-negative matrix *V* having n by m dimensions then, we find non-negative matrix factors *W* and *H* such that,

$$\boldsymbol{V = W.H} \qquad \textbf{(1)}$$

Such that *W* and *H* are factorized into *n by r* and *r by m* dimensions respectively. Here, $r < m$ and $r < n$. Hence, the resultant *W* and *H* would be converted into a smaller dimension than *V* and compresses the original data matrix *V*.

The factorization of $V = W.H$ is based on the principle of optimization where the cost function is defined so as to quantify the quality of the approximation. The cost function is constructed so as to minimize the square of Euclidean distance between *V* and *W.H*. Then, the cost function can be written as,

$$J = \|V - W.H\|^2 \qquad (2)$$

In simple words, the aim of the cost function ($J$) is to minimize the residual between $V$ and $W.H$. Now, the number of features are extracted from the original data based on satisfactory amount of variance explained by certain number of smaller dimensions. Then, the total variance accounted for can be determined as,

$$VAF = 100 \times (1 - \frac{SSE}{SST}) \qquad (3)$$

where, $SSE$ = sum of the squared residual, i.e., sum of square of $V - W.H$

$SST$ = sum of squared original dataset, i.e., sum of square of $V$

As we can see that this method is quite compatible for extraction of the muscle modes. Here V can be constructed as the EMG dataset for n muscles with m number of trials. Then W can be decomposed as having n muscles by r number of synergies with H being r synergies with m number of trials. Therefore, column of W would represent the weight of each of the muscles towards that r number of synergies. Finally, number of synergies (r) can be extracted based on the VAF.

### *2.2. Principal component analysis (PCA)*

Principal component analysis (PCA) is one of the factor analysis technique used for dimension reduction through orthogonal transformation (Wold, Esbensen, & Geladi, 1987). The premise behind this analysis is that if we have a matrix $P$ of $n$ *by* $m$ dimensions, then it helps determine a covariance relationship between the variables within the matrix $P$ in terms of fewer uncorrelated and unobservable variables termed as factors. This explanation of the covariance relationship is possible through variance-covariance structure through linear combinations of the original variables. Here the n by m variable can be possibly explained by smaller number of new variables $r$ then, the $m$ variables can be replaced by $r$ which are known as the principal components ($PCs$). In case of the postural control, $P$ matrix contains activation of $m$ muscles over $n$ observations. Then, there exists an $i^{th}$ component, $PC_i$ is given by

$$PC_i = e_i.P \qquad (4)$$

where *e*, which is eigenvectors, consists of the coefficient for the principal components where *i = 1,2,….,m*. The PCs are known as muscle modes or M-modes which are the jointly activated muscle groups for a particular task.

Here, the coefficients of the first PC is selected so as to maximize the variance accounted by the data within that PC followed by a second PC orthogonal to first PC with the following maximal variance. This process is continued until the number of PCs are selected accounting for satisfactory amount of variance from the transformed data. In some cases, the interpretation of PCs might be difficult in which case these components are rotated for better interpretation. The selection is also based on the Kaiser's criterion which is based on the eigenvalue of *e* (*eigenvalue > 1*). Based on this criterion, eigenvalue being greater than one for a PC means that that PC would have enough variance to explain behavior of at least one muscle (Kaiser, 1962). For each PC, the muscles are given weights or loadings based on its closeness from the PC which is constrained to be a unit vector.

# 3. Physiological nature of multi-element synergies

## *3.1. Concept of synergy*

In motor control literatures the term synergy has been often used with each group of researchers with their own unique interpretation. In layman's term 'synergy' can be simply understood as 'working together'. The first person to introduce the term would be Hughlings Jackson who even though did not use the term synergy, postulated that muscles work in a groups to perform a certain task and are not independent (Jackson, 1889). As mentioned above, Bernstein was first to introduce synergy as a solution to the problem of excessive degrees of freedom. He suggested that the human postural control system has been divided into four level (A, B, C and D). Level-A: muscle tone, Level-B: muscular and articular links, Level-C: level of space and Level-D: level of actions. Here, Level-B was postulated to be the level of synergies where interaction between the elements performing a certain task occurs (Nikolai Bernstein, 1966). Hence, synergy can be understood as a task-specific phenomenon i.e., for a certain problem CNS would recruit the elements in groups

depending on the specificity of the problem to find an effective solution (Gelfand & Latash, 1998; Latash et al., 2002). Hence, to understand the interaction among the elements to perform a certain task, a functional meaning must be portrayed to the interaction among the elements depending on the context of the task. Therefore, there are several theories proposed to understand the interaction among the elements involved in a certain task and a further description of these theories are in the following sections.

### *3.2. Uncontrolled manifold (UCM)*

One of the studies involving postural synergy was performed by Danna-dos-Santos where they performed postural sway task (Danna-dos-Santos, Slomka, Zatsiorsky, & Latash, 2007). They aimed to determine the synergistic muscle interaction in control of COP in Anterior-Posterior direction. They used the uncontrolled manifold hypothesis (UCM hypothesis) approach to explore the synergistic features of the directional postural system. This method was initially developed by Scholz and Schoner where they conducted a study involving motor synergies using kinematics as variables of interest. The UCM hypothesis postulated that the controller (CNS) acts in the space of elemental variables (e.g., joint angles, muscles, finger forces, etc.) to create synergies that would stabilize certain important performance variable (Park, Zatsiorsky, & Latash, 2010; Scholz & Schöner, 1999).

In case of the postural control, when the controller aims to stabilize center of pressure (COP) through utilization of activity of multiple muscles, it strives to select a subspace within the space of muscle activity corresponding to the desired value of COP. The subspace within the space of muscle activity is the uncontrolled manifold. In case of the study performed by Danna-dos-Santos, they determined the muscle activity via EMG during directional movement task into a normalized time scale and analysed the variability found across the trials. The variability was then decomposed into two components (Danna-dos-Santos et al., 2007; Krishnamoorthy et al., 2003):

1) *VUCM:* Variability component parallel to the uncontrolled manifold and does not affect the performance variable.

2) *VORT:* Variability component orthogonal to the uncontrolled manifold and affects the performance variable.

Analyzing this variability is the core concept behind the UCM hypothesis. It helps us determine the existence, strength and quantify the development of new synergy. Hence, the UCM approach was used to determine coordination among muscle activation patterns to stabilize the COP during directional postural sway task. That is, the CNS organizes the muscle coordination in such a manner that the co-variation among the muscles would stabilize the endpoint COP. Therefore, repetitive attempts at stabilization of COP would result in reduction on variance of the space orthogonal to the manifold when compared to the actual manifold. However, due to large number of muscles involved in control of posture during certain directional postural sway task, the muscles were grouped together into independent components where a group of muscles would be independent of another group depending of specific value of COP. These sets of independent components were termed as muscle modes (Danna-dos-Santos et al., 2007; Krishnamoorthy et al., 2003). The muscle modes are hypothetical latent variables, observed at behavioral level, corresponding to desired involvement of certain group of muscles into COP control task.

Hence, Danna-dos-Santos determined that during voluntary sway in anterior direction dorsal muscles would group together and during posterior directional sway anterior muscles would group together to stabilize the COP. Hence, the CNS would unite the muscles in a certain functional groups with the aim of stabilizing the COP (Danna-dos-Santos et al., 2007). The reasonability of the results using this method makes it a reliable candidate in understanding postural synergies. Therefore, the same approach can be utilized in the studies involved in this dissertation where isometric control of muscles are required to stabilize the variability in COP.

# III. Experimental Protocol and Data Analysis

## 1. Methods

### *1.1. Subjects*

Eight healthy subjects, 6 male and 2 female (age = 29.13 ± 4.32 years, body mass = 65.50 ± 7.22 kg, height = 1.70 ± 0.58 m) were recruited for the study. These subjects were right side dominant with no known neurological and muscular disorder in both their upper and lower extremities. The subjects signed a consent form indicating the procedures and potential risks involved during the experiment in accordance to the ethical standards set by Institutional Review Board of Seoul National University.

### *1.2. Equipment*

Force platform (AMTI force-platform, Model no. MC3A-1000, Advanced Mechanical Technology, Inc., New York, USA) was used to record 3 directional forces ($F_X$, $F_Y$, $F_Z$) and moments of forces ($M_X$, $M_Y$, $M_Z$) at a sampling frequency of 1000 Hz. The coordinates of the force plate was set so that X, Y and Z axes denoted motion in Anterior-Posterior (AP), Medial-Lateral (ML) and Superior-Inferior (SI) directions respectively. A monitor was set up at about .m from the force plate where the real-time feedback of the AP and ML coordinates of the COP ($COP_{AP}$ and $COP_{ML}$ respectively) was provided in it. 8 infrared motion analysis cameras (Oqus 500, Qualisys AB, Sweden) were utilized to record 22 anatomical markers (Figure 1) at a sampling frequency of 100 Hz was used to calculate lower extremity joint angles. Surface EMG (Trigno$^{TM}$ Wireless Systems, Delsys Inc., USA) was used to record the muscle activity of 11 leg and trunk muscles from the right side of the body: Erector Spinae (ES), Rectus Abdominis (RA), Rectus Femoris (RF), Vastus Lateralis (VL), Vastus Medialis (VM), Biceps Femoris (BF), Semitendinosus (ST), Gastrocnemius Lateralis (GL), Gastrocnemius Medialis (GM), Soleus (SOL) and Tibialis Anterior (TA). The sampling frequency of EMG signal was 2000 Hz. Force Platform data was collected via customized Labview program

(Labview 2015, National Instruments, Texas, USA). EMG data was collected via EMG acquisition program (EMG Acquisition, Delsys Inc., USA) and kinematic data was collected via Qualysis Track Manager(Qualisys Track Manager, Qualysis AB, Sweden). All three systems were synced together using a sync box.

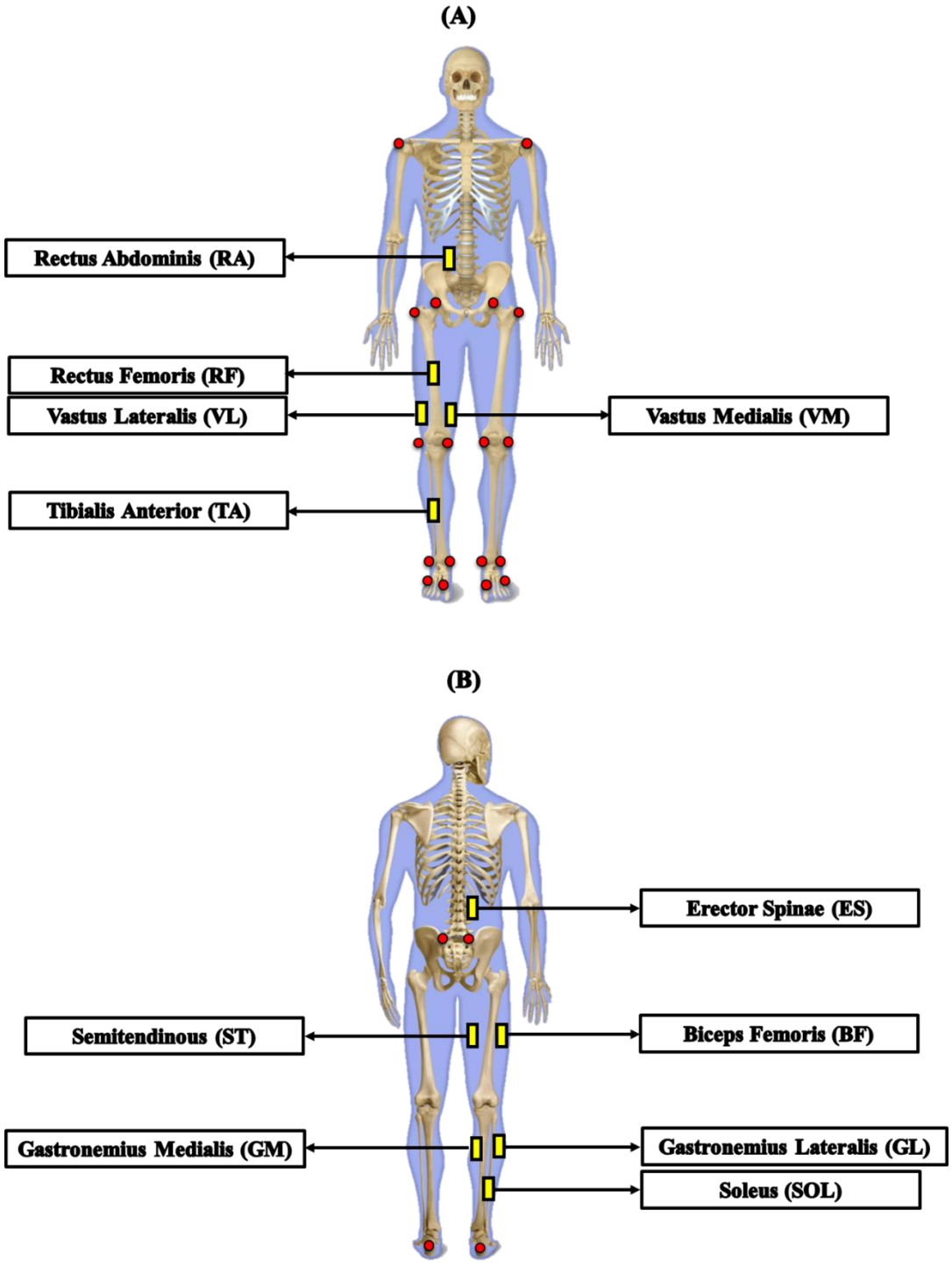

**Figure 1:** EMG and reflective marker placement position for the experiment (A) Frontal View & (B) Dorsal View. Yellow squares denotes EMG sensors and red circles denotes reflective markers. ES = Erector Spinae, RA = Rectus Abdominis, RF = Rectus Femoris, VL = Vastus Lateralis, VM = Vastus Medialis, BF = Biceps Femoris, ST = Semitendinous, GL = Gastronemius Lateralis, GM = Gastronemius Medialis, SOL = Soleus & TA = Tibialis Anterior.

### *1.3. Experimental procedure*

Figure-2 demonstrates the experimental setup. Prior to the actual experiment, subjects were given enough time to get familiarized with the experimental procedures. Following that, subjects were asked to stand barefoot on the force platform with their arms crossed on their shoulder and narrow stance was maintained between the feet keeping the distance between the fibula joints is set at 5 cm. The COP data from the subject's foot position was extracted and displayed on a customized feedback screen developed using Labview. The whole experimental procedure was divided into two tasks: I) Preliminary Task and II) Main Task

A preliminary task included determination of the subject's Maximal Voluntary Displacement (MVD), which is the maximal distance achievable through voluntary postural sway of the body using ankle strategy (movement performed by motion around the ankle joint while minimizing motion at the knee and hip joints). MVD was determined separately for four directions: Anterior (Forward), Posterior (Backward), Medial (Left) and Lateral (Right). This was achievable by moving the feed backed COP position slowly following an auditory metronome set at a frequency of 0.33 Hz. A total of 3 trails were performed for this task with each trail lasting 10 seconds. Average of these 3 trials were considered as the MVD of each subject.

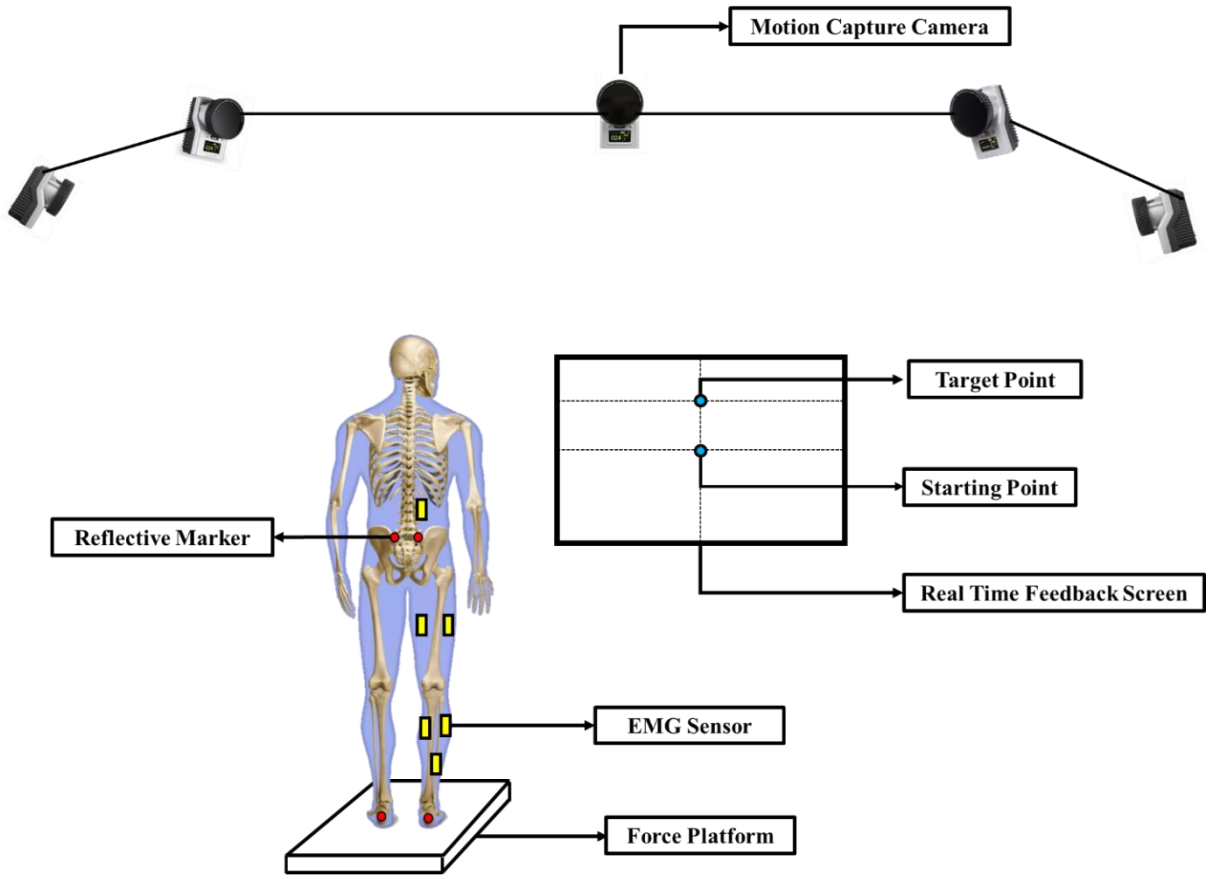


**Figure 2:** An illustration of the experimental setup. Participants are standing on a force platform. Real time visual feedback screen shows the starting point and the target point (80% of MVD).

The main task was a multi-directional voluntary postural body sway. Similar to the preliminary task, the subjects were asked to stand barefoot on the force platform in the above mentioned stance. The customized feedback screen displayed a point representing 80% of MVD of each subject in the aforementioned four directions separately. Following auditory metronome set at a frequency of 0.33 Hz, subjects were asked to slowly move their COP trajectory to that point using ankle strategy. Once subjects arrived to that point, they were asked to maintain the position for 10s before returning back to their original position. Each trail was performed for 20s with a total of 15

trials for each direction. Hence, the total number of trails was 60 (4 directions × 15 trials). The validity of the ankle strategy was determined using the kinematic data by analyzing the deviation of hip, knee and ankle joint angles.

## 2. Data analysis

The signals obtained during the experiment were processed offline via a customized MATLAB program. Firstly, all of the signals were resampled to 1000 Hz. The data obtained from the main task was divided in two phases:

I) *Dynamic Phase*: The data from time of sway initiation to the time of contact with the 80% MVD point.

II) *Quasi-Static Phase*: The data from 2.5 seconds after contact with the 80% MVD point to the data 2.5 seconds before returning to the sway initiation position.

All the signals were separated according to these phases.

The kinematic data obtained from motion capture system was filtered using zero-lag $2^{nd}$ order low-pass Butterworth filter with a cut-off frequency of 6 Hz. The COP data obtained from the force platform was filtered using zero-lag $4^{th}$ order low-pass Butterworth filter with a cut-off frequency of 10 Hz. The data obtained for two phases was time normalized to 100% for each trial so that the two phases would be converted into a definite and comparable sway cycle (0% - 100%).

### *2.1. Joint angles*

The joint angles calculated here is the relative joint angles between the two segments which is done through human modelling program, Visual 3d (C-Motion, Inc., USA). The joint angles calculated here are determined in order to confirm the utilization of ankle strategy. Hence, flexion/ extension and adduction/abduction angles are calculated across the experimental cycle for hip, knee and ankle joints. Hence, minimum deviation of the joint angles must be observed for hip and knee joints with significantly larger deviation around the ankle. For anterior/posterior direction, the deviation around ankle is observed for flexion/extension angle whereas, for medial/lateral direction sway, the deviation around ankle is observed for abduction/adduction angle.

For joint angle calculation equations (5) and (6) were utilized,

If ($X_1$, $Y_1$, $Z_1$), ($X_2$, $Y_2$, $Z_2$) and ($X_3$, $Y_3$, $Z_3$) is the position of the marker defining the position of center of a hip, knee and ankle joints respectively then,

$$\begin{aligned} a_1 &= \sqrt{(X_3 - X_2)^2 - (Z_3 - Z_2)^2} & a_2 &= \sqrt{(Y_3 - Y_2)^2 - (Z_3 - Z_2)^2} \\ b_1 &= \sqrt{(X_2 - X_1)^2 - (Z_2 - Z_1)^2} & b_2 &= \sqrt{(Y_2 - Y_1)^2 - (Z_2 - Z_1)^2} \\ c_1 &= \sqrt{(X_1 - X_3)^2 - (Z_1 - Z_3)^2} & c_2 &= \sqrt{(Y_1 - Y_3)^2 - (Z_1 - Z_3)^2} \end{aligned} \quad \textbf{(5)}$$

Then, relative joint angles was calculated using law of cosines such that,

$$\begin{aligned} \theta_{flex/ext} &= cos^{-1}\left(\frac{a_1^2 + b_1^2 - c_1^2}{2a_1b_1}\right) \\ \theta_{abd/add} &= cos^{-1}\left(\frac{a_2^2 + b_2^2 - c_2^2}{2a_2b_2}\right) \end{aligned} \quad \textbf{(6)}$$

where,

$\theta_{flex/ext}$ : flexion/extension angle with positive indicating flexion whereas, negative values indicating extension.

$\theta_{abd/add}$ : abduction/adduction angle with positive indicating abduction whereas, negative values indicating adduction.

### *2.2. EMG processing*

Initially, in order to compensate for the electromechanical delay, EMG signal was shifted 50-ms with respect to the data obtained from the force platform. Raw EMG signals were then notch filtered at 60 Hz to remove any noise emulating from any electrical devices present in the laboratory. The signals were then rectified and band-pass filtered using a zero-lag 4$^{th}$ order band-pass filter with cutoff frequencies between 20 Hz and 350 Hz. Further, since our experiment is concerned with

relatively slow changes in muscle activity (EMG signal), a moving average filter was implemented within a time window of 100-ms. Filtered EMG signals were integrated over a 1% time window of the sway cycle which is denoted as *IEMG*. For comparison of *IEMG* value across subjects, the *IEMG* was normalized by the maximal EMG value ($IEMG_{MAX}$). The $IEMG_{MAX}$ was determined by stacking all the filtered EMG data from the 15 trials and integrated it over 1% time window and selected the maximum value for each muscle. Hence, normalized IEMG data is calculated using equation (7),

$$IEMG_{NORM} = \frac{IEMG}{IEMG_{MAX}} \quad \textbf{(7)}$$

The $IEMG_{NORM}$ was constructed into a matrix with 11 columns corresponding to 11 muscles and 1500 rows corresponding to $IEMG_{NORM}$ value stacked for a total of 15 trials for each direction.

### *2.3. Determination of M-modes using non-negative matrix factorization (NMF)*

From our dataset, the transpose of previously mentioned *6000 by 11* matrix $IEMG_{NORM}$ data was taken as the original V converting it into a *11 by 6000* matrix where *11* is the number of muscles and *6000* is the number of observations. Then, it is reconstructed into a *W.H* matrix where *W* is considered as the M-modes which is decomposed into *11 by r* matrix where *r* is the number of factors or in our case number of M-modes. The selection of M-modes is based on the amount of *VAF* being greater than 90% (*VAF > 90%*).

### *2.4. Determination of M-modes using principal component analysis (PCA)*

In our study, $IEMG_{NORM}$ data was utilized to group muscles depending upon the parallel scaling of the activation levels of the muscles during a multi-directional voluntary postural sway task and these groups of muscles are defined as M-modes. We are interested in M-modes in all 4 directions so, we stacked $IEMG_{NORM}$ data into a *6000 by 11* matrix containing $IEMG_{NORM}$ data from all 4 directions in the following sequence: anterior-posterior-medial-lateral. The M-modes were determined through PCA analysis which was varimax rotated. This allows reduction of the 11-dimensional muscle space into a smaller dimensional space (M-Mode space). The extraction of the number of M-modes based on the Kaiser criterion (*eigenvalue >1*). In our study, the number of extracted modes

was determined to be 3. In addition, the weights of each muscle for M-mode was found to be significant for loading value > 0.4.

### *2.5. Determination of jacobian matrix*

The linear relationship between small changes in the elemental variables with the performance variable was used to estimate the Jacobian of the system. The elemental variables is M-modes (*ΔM*) and performance variable is center of pressure (*ΔCOP*) for our analysis. Similar to the EMG dataset, COP was also stacked into a *6000 by 1* matrix containing the COP data from all 4 directions. The linear relationship is determined using multiple regression analysis and the coefficients obtained from equation (8) and (9) was used to form the Jacobian matrix.

$$\Delta COP = K_1 \Delta M_1 + K_2 \Delta M_2 + K_3 \Delta M_3 \quad \textbf{(8)}$$

Then,

$$Jacobian\ Matrix: J = [K_1\ K_2\ K_3]^T \quad \textbf{(9)}$$

### *2.6. UCM analysis: determination of index of multi-muscle synergy*

The primary aim of the UCM analysis is to determine the coordination of the muscles in order to stabilize the COP during multi-directional voluntary postural sway task. The UCM approach allows an analysis of the variance found in the M-mode space and determine if it is value to a stable COP value which is reproducible over each sway cycle. Here, *ΔM* has a dimensionality of 3 (*n=3*) and co-variation among these M-modes are assumed to stabilize particular magnitude of *ΔCOP* which has dimensionality of 1 (*d=1*). Hence, this system is redundant while stabilizing the *ΔCOP*. Since, we are assuming that there is a linear relationship between *ΔM* and *ΔCOP*, the mean magnitudes of the *ΔM* was determined and is subtracted from the computed *ΔM* with residuals used for further analysis.

UCM approach here helps determine if the M-modes are consistent over sway cycles and reproduce a stable value of COP. Hence, UCM space was calculated as the null space of the corresponding Jacobian. This null space can be defined as set of vectors $X$ such that it satisfies the set of equations $JX = 0$. Then, the null space is spanned by basis vectors, $E_j$, The demeaned value of $\Delta M$ is then projected onto this null space such that,

$$F_{UCM} = \sum_{j=1}^{n-d}(E_j^T.(\Delta M))E_j \quad \textbf{(10)}$$

And the component orthogonal to the null space is denoted by,

$$F_{ORT} = (\Delta M) - F_{UCM} \quad \textbf{(11)}$$

Then, the amount of variance per DOF within the UCM space is denoted by,

$$V_{UCM} = \frac{\sum_{trials}F_{UCM}^2}{(n-d)N_{trials}} \quad \textbf{(12)}$$

And variance per DOF within the space orthogonal to the UCM space is denoted by,

$$V_{ORT} = \frac{\sum_{trials}F_{ORT}^2}{dN_{trials}} \quad \textbf{(13)}$$

Finally, the normalized differences between these variances is denoted by,

$$\Delta V = \frac{V_{UCM}-V_{ORT}}{V_{TOTAL}} \quad \textbf{(14)}$$

where, $V_{TOTAL}$ is the total variance accounted per degree of freedom. Hence, if $\Delta V > 0$, i.e., $V_{UCM} > V_{ORT}$, negative co-variation among the individual M-modes exists, which is interpreted as the evidence of COP stabilizing synergy. If $\Delta V = 0$, there exists independence in variation of M-modes, whereas, $\Delta V < 0$ would indicate existence of positive co-variation among the individual M-modes. A detailed explanation can be found in (Latash et al., 2007).

### *2.7. Similarity index*

The similarity index on context of present research is utilized to determine the similarity between the M-modes extracted from the PCA and NMF across subjects. This index stems from the

theory of cosine similarity which is a measure of similarity between two non-zero vectors by calculating cosine angle between a representative vector and individual vectors under evaluation. In the context of PCA and NMF analysis, the representative vector would be the central mode vector ($C$) which is the average vector across subjects and individual vector is the M-mode vector ($M_i$) for individual subject across the 11-dimensional muscle space. Here, $i$ is the number of subjects. Hence, the cosine of the angle between the $C$ and $M_I$ and thereby similarity index is measured using equations (15) and (16),

Firstly, the cosine of $C$ and $M_i$ is derived using Euclidean dot product between the vectors:

$$\boldsymbol{M_i.C = \|M_i\| \|C\| cos\theta} \quad \textbf{(15)}$$

Hence, the similarity index is using the dot product and magnitude of the two vectors,

$$\boldsymbol{Similarity\ Index = cos\theta = \frac{M_i.C}{\|M_i\| \|C\|} = \frac{\sum_{j=1}^{n}(M_i)_n C_n}{\sqrt{\sum_{j=1}^{n}(M_i)_n{}^2}\sqrt{\sum_{j=1}^{n}C_n{}^2}}} \quad \textbf{(16)}$$

where $n$ is the number of muscles.

The value of the similarity index ranged from 0 to 1. If similarity index is equal to 1, the two vectors were deemed parallel (same) whereas, if similarity index is equal to 0, the two vectors were deemed orthogonal (opposite).

## 3. Statistics:

Data are presented as mean ± standard errors (SE). Significant activation/loadings for muscle modes were selected to be greater than *0.4*. One-way ANOVA was used to determine differences in MVD and synergy index setting factor as direction for both. Independent t-test was utilized to determine significant differences in degrees of freedom between methods. Significance value was set at $p < 0.05$.

# IV. Results

## 1. Maximal voluntary deviation (MVD) & joint angles

The maximal voluntary deviation (MVD) in posterior direction was higher compared to other directions (Figure 3). There was statistically significant difference between mean MVD as determined by one-way ANOVA [$F(3, 28) = 11.001$, $p < 0.05$]. Post hoc comparisons using Tukey HSD test indicated that mean MVD was significantly higher for anterior direction compared to other directions.

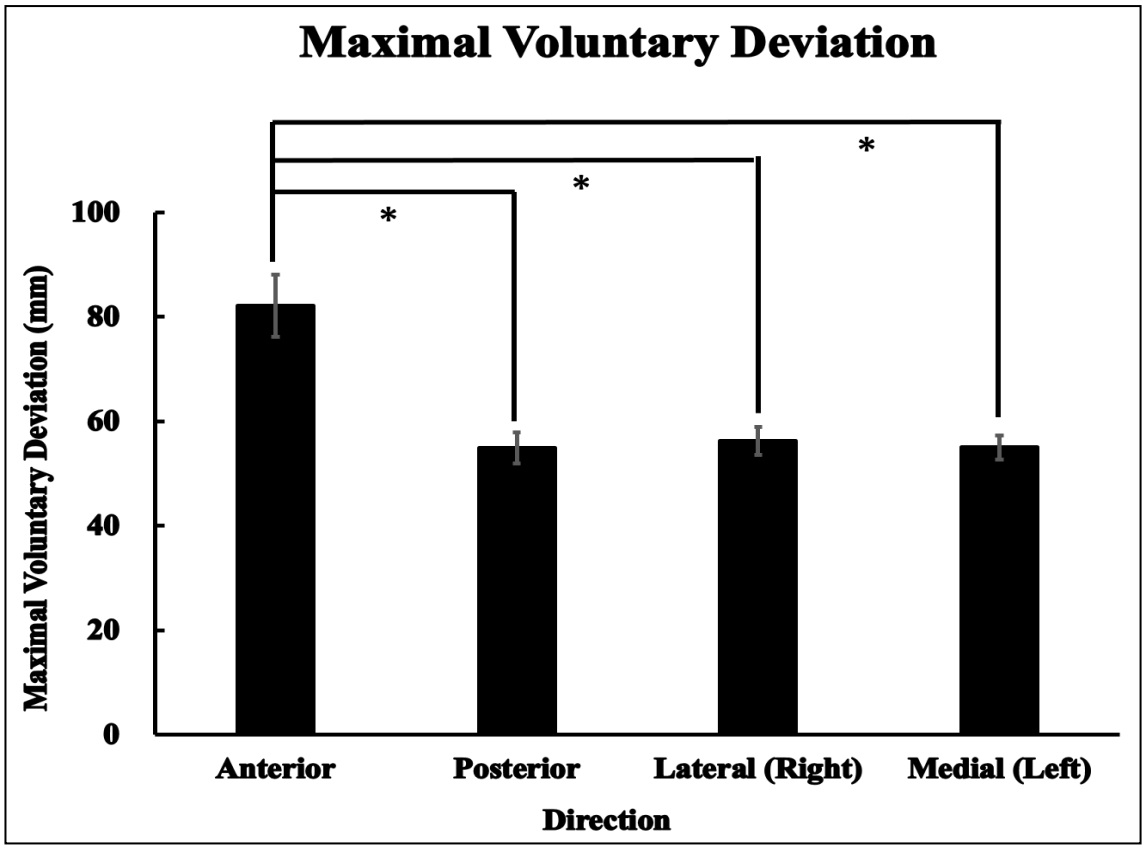


**Figure 3:** Average (±SE) COP travel distance across subjects from initial position to 80% MVD target point.

* indicates statistical significance.

The maximal deviation of the flexion/extension & adduction/abduction joint angles from the initial position to throughout the experimental cycle was determined. It was determined that for all directions deviation of the joint angles was primarily observed around the ankle (Figure 4).

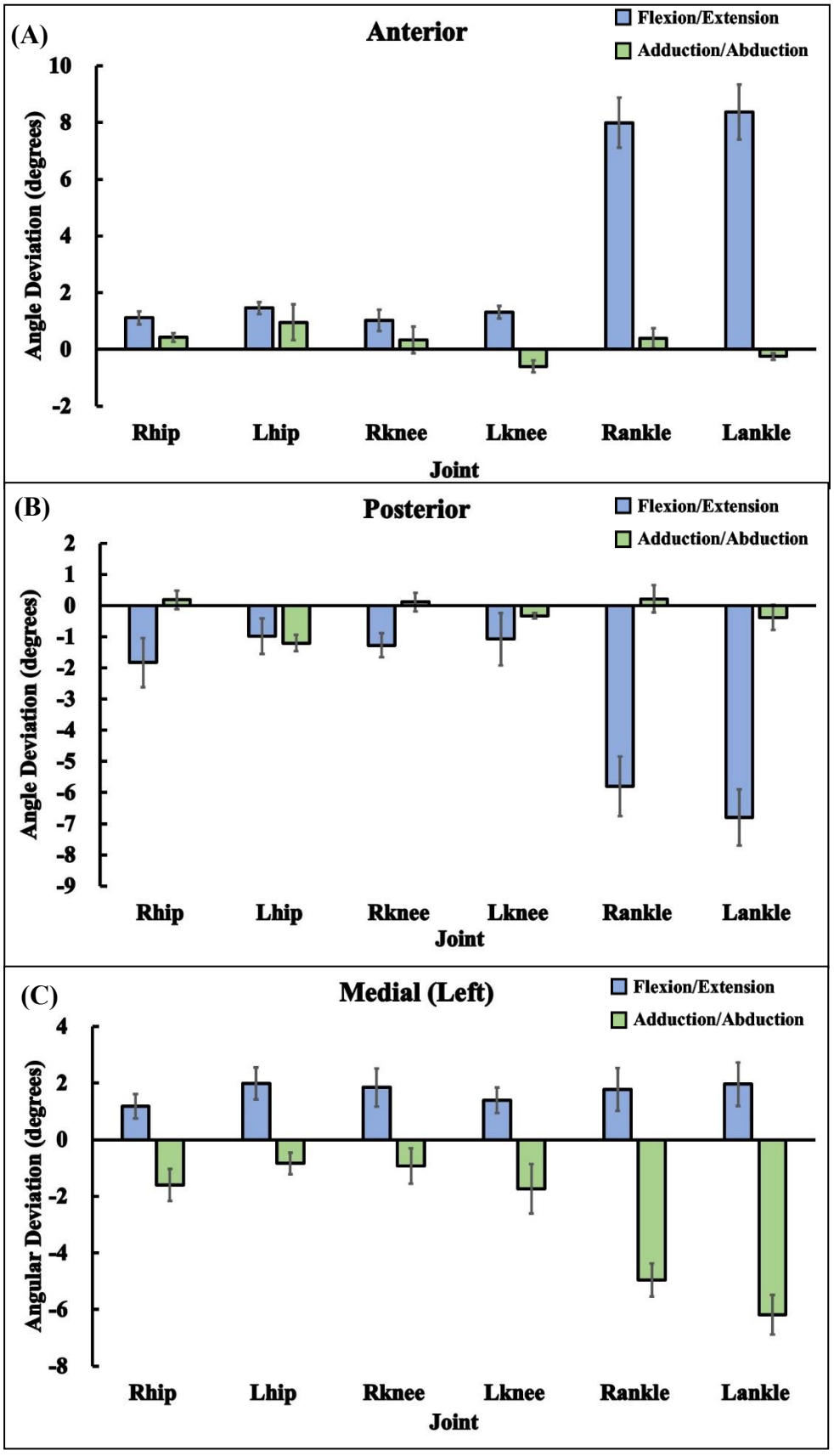

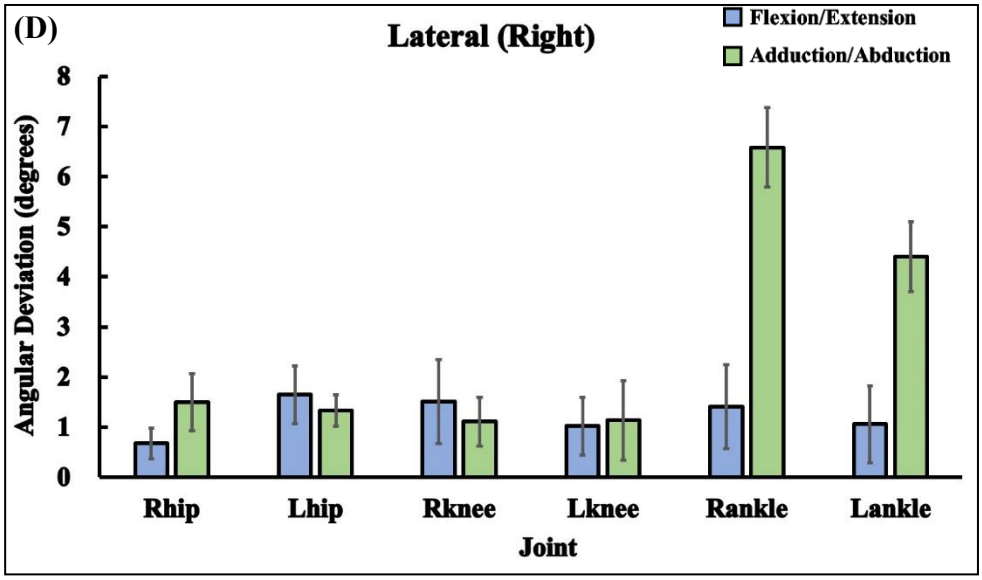


**Figure 4:** Average (±SE) flexion/extension and adduction/abduction angles across subjects for hip, knee and ankle for left and right extremity in (A) Anterior, (B) Posterior, (C) Medial (Left) and (D) Lateral (Right). Rhip = Right hip joint angle, Lhip = Left hip joint angle, Rknee = Right knee joint angle, Lknee = Left knee joint angle, Rankle = Right ankle joint angle & Lankle = Left ankle joint angle.

## 2. M-modes

### *2.1. Non-negative matrix factorization (NMF)*

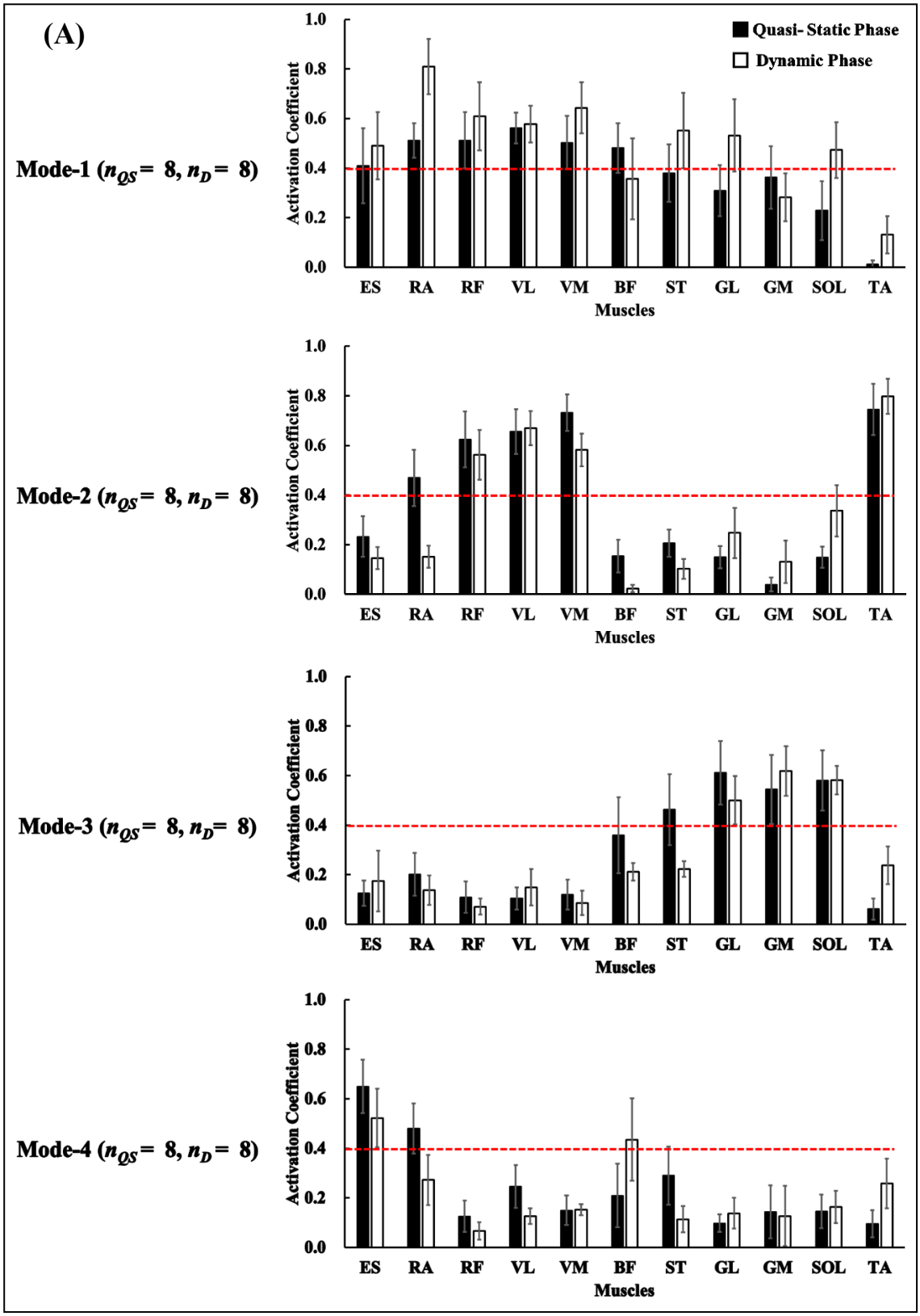

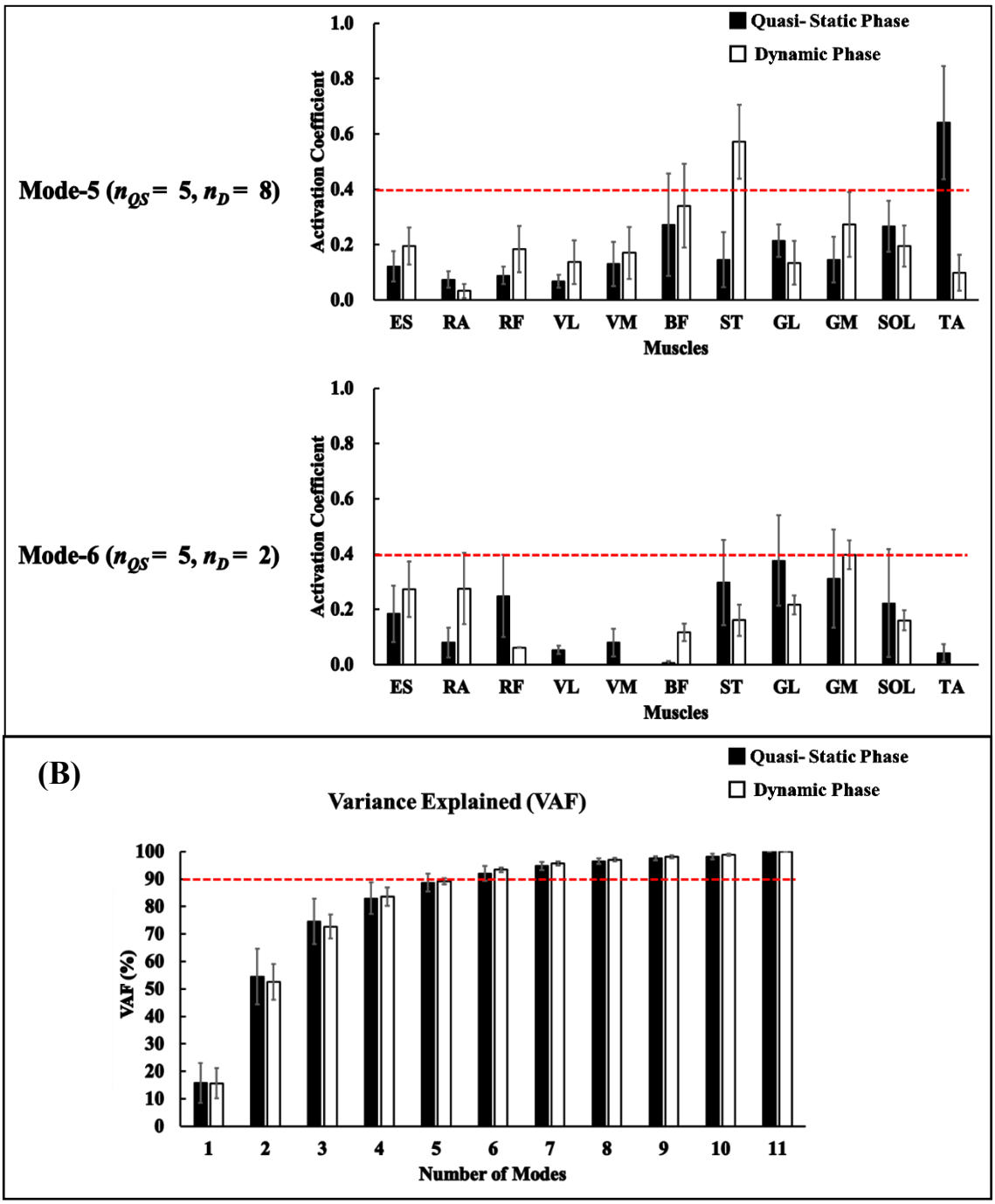


**Figure 5:** Average (±SE) across subjects (A) activation coefficient of each mode and (B) variance explained by each mode for both phases. ES = Erector Spinae, RA = Rectus Abdominis, RF = Rectus Femoris, VL = Vastus Lateralis, VM = Vastus Medialis, BF = Biceps Femoris, ST = Semitendinous, GL = Gastronemius Lateralis, GM = Gastronemius Medialis, SOL = Soleus & TA = Tibialis Anterior.

*Significance value of activation coefficient > 0.4 & variance explained > 90%. $n_{QS}$ : number of subjects in a mode for quasi-static phase & $n_D$ : number of subjects in a mode for dynamic phase.

Based on our criterion (*VAF > 90%*), for quasi-static and dynamic phases, on average *5.25 ± 1.04* and *5.25 ± 0.46* modes were extracted respectively (Figure 5(B)). Here, we looked at the maximum amount of modes extracted by any of the subjects which in our case is six. The average amount of variance across subjects explained by each mode and all modes is shown for both phases in Table 2 and Figure 5(B).

**Table 2:** Average variance accounted for (±SE) across subjects by each mode and overall modes for PCA.

| ***Phase*** | ***Quasi - Static*** | ***Dynamic*** |
|---|---|---|
| ***Mode - 1*** | 15.80±7.30 % | 15.64±5.49 % |
| ***Mode - 2*** | 38.64±9.85 % | 36.91±7.56 % |
| ***Mode - 3*** | 20.12±6.31 % | 20.17±3.41 % |
| ***Mode - 4*** | 8.47±3.21 % | 10.91±2.15 % |
| ***Mode - 5*** | 5.75±3.12 % | 5.55±2.74 % |
| ***Mode - 6*** | 3.26±0.87 % | 4.24±0.54 % |
| ***Total*** | ***90.34±1.61 %*** | ***90.23±1.88 %*** |

Figure 5(A) shows the activation coefficients of the muscles for the six modes across subjects. Based on the criterion (*activation coefficient > 0.4*), for both phases, a large number of muscles significantly activated with which were different for quasi-static (*ES, RA, RF, VL, VM & BF*) and dynamic (*ES, RA, RF, VL, VM, ST, GL & SOL*) phases for first mode. Additionally, other muscles were also mildly activated with the exception of TA but were not significantly activated based on our criterion. Ventral muscles (*quasi-static: RA, RF, VL, VM & TA and dynamic: RF, VL, VM & TA*) significantly activated for the second mode and was similar for both phases. Dorsal muscles (*quasi-static: ST, GL, GM & SOL and dynamic: GL, GM & SOL*) significantly activated for the third mode and was similar for both phases. Trunk muscles (*ES & RA*) significantly activated for quasi-static phase whereas, *ES & BF* was significantly activated for the dynamic phase on the fourth mode. *TA & ST* was significantly activated for quasi-static and dynamic phase respectively on the fifth mode. Finally, there was no significant activation for the sixth mode with moderate activation for few of the muscles for both phases.

The above mode results from the non-negative matrix factorization is confirmed by the general directional activation of the muscles. Based on these results we can say that muscles with significant activation in the six modes is seen in Table 3:

**Table 3:** Table showing the muscles activated for the mode depending on phases and naming of each mode for PCA.

| ***Mode*** | ***Phase*** | ***Muscles Involved*** | ***Mode Name*** |
|---|---|---|---|
| ***Mode - 1*** | ***Quasi - Static*** | ES, RA, RF, VL, VM & BF | Broad Activation |
| | ***Dynamic*** | ES, RA, RF, VL, VM, ST, GL & SOL | Broad Activation |
| ***Mode - 2*** | ***Quasi - Static*** | RA, RF, VL, VM & TA | Forward Dominant |
| | ***Dynamic*** | RF, VL, VM & TA | Forward Dominant |
| ***Mode - 3*** | ***Quasi - Static*** | ST, GL, GM & SOL | Back/ Left/ Rightward Dominant |
| | ***Dynamic*** | GL, GM & SOL | Back/ Left/ Rightward Dominant |
| ***Mode - 4*** | ***Quasi - Static*** | ES & RA | Trunk Dominant |
| | ***Dynamic*** | ES & BF | Backward Dominant |
| ***Mode - 5*** | ***Quasi - Static*** | TA | TA Dominant |
| | ***Dynamic*** | ST | ST Dominant |
| ***Mode - 6*** | ***Quasi - Static*** | None | Limited Activation |
| | ***Dynamic*** | None | Limited Activation |

ES = Erector Spinae, RA = Rectus Abdominis, RF = Rectus Femoris, VL = Vastus Lateralis, VM = Vastus Medialis, BF = Biceps Femoris, ST = Semitendinous, GL = Gastronemius Lateralis, GM = Gastronemius Medialis, SOL = Soleus & TA = Tibialis Anterior.

The naming of the modes were based on the parallel changes in muscle activity with respect to displacement of the center of pressure and also the general activation of the muscles.

*2.2. Principal component analysis (PCA)*

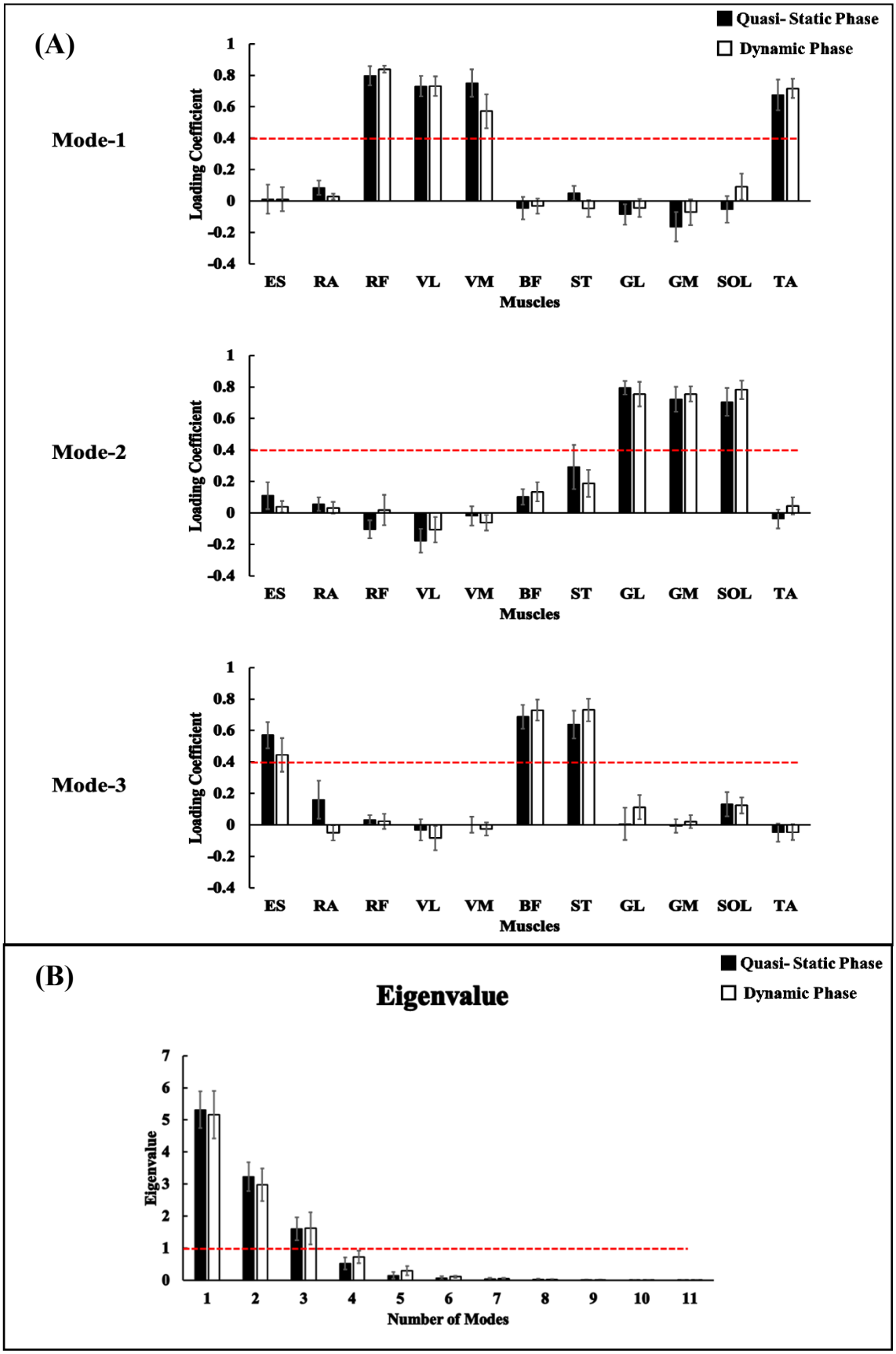

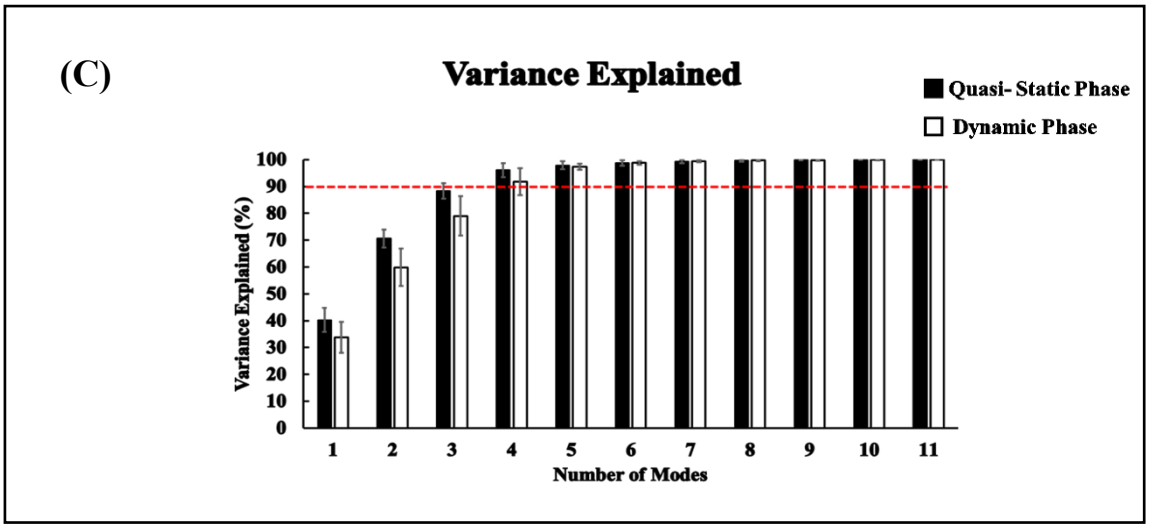


**Figure 6:** Average (±SE) across subjects (A) loading coefficient, (B) eigenvalue and (C) variance explained by each mode for both phases. ES = Erector Spinae, RA = Rectus Abdominis, RF = Rectus Femoris, VL = Vastus Lateralis, VM = Vastus Medialis, BF = Biceps Femoris, ST = Semitendinous, GL = Gastronemius Lateralis, GM = Gastronemius Medialis, SOL = Soleus & TA = Tibialis Anterior.

*Significance value for loading coefficient > 0.4, eigenvalue > 1 & variance explained > 90%.

Based on our criterion (*eigenvalue >1*), *3 modes* were extracted for both phases across subject (Fig. 6(B)). The average amount of variance across subjects explained by each mode and all three modes is shown for both phases in Table 4 and Figure 6(C).

**Table 4:** Average variance explained (±SE) across subjects by each mode and overall modes for PCA.

| ***Phase*** | ***Quasi - Static*** | ***Dynamic*** |
|---|---|---|
| ***Mode - 1*** | 39.55±4.16 % | 33.27±5.95 % |
| ***Mode - 2*** | 30.92±2.14 % | 25.88±3.61 % |
| ***Mode - 3*** | 17.48±3.93 % | 19.26±3.83 % |
| ***Total*** | ***88.31±2.94 %*** | ***79.03 ±7.27 %*** |

Figure 6(A) shows the loading coefficients of the muscles for the three modes across subjects. Based on our criterion (*loading coefficient > 0.4*), ventral muscles (*RF, VL, VM & TA*) predominantly loaded significantly on the first mode. The dorsal muscle specifically situated at the shank (*GL, GM & SOL*) loaded significantly on the second mode. The dorsal trunk muscle and hamstring muscles (*ES,*

*BF & ST*) were significantly loaded on the third mode. *RA* was not significantly loaded on any of the modes which is confirmed by the lack of its activation in any of the four directions except a slight increment during sway in anterior direction. All of these results were similar for both phases.

The above mode results from the principal component analysis is confirmed by the general directional activation of the muscles. Based on these results we can say that muscles with significant loading in the three modes were (Table 5):

**Table 5:** Table showing the muscles activated for the mode depending on phases and naming of each mode for PCA.

| ***Mode*** | ***Phase*** | ***Muscles Involved*** | ***Mode Name*** |
|---|---|---|---|
| ***Mode - 1*** | ***Quasi - Static*** | RF, VL, VM & TA | Push - Forward |
| | ***Dynamic*** | | |
| ***Mode - 2*** | ***Quasi - Static*** | GL, GM & SOL | Push - Back/ Left/ Rightward |
| | ***Dynamic*** | | |
| ***Mode - 3*** | ***Quasi - Static*** | ES, BF & ST | Push - Backward |
| | ***Dynamic*** | | |

ES = Erector Spinae, RA = Rectus Abdominis, RF = Rectus Femoris, VL = Vastus Lateralis, VM = Vastus Medialis, BF = Biceps Femoris, ST = Semitendinous, GL = Gastronemius Lateralis, GM = Gastronemius Medialis, SOL = Soleus & TA = Tibialis Anterior.

The naming of the modes were based on the parallel changes in muscle activity with respect to displacement of the center of pressure and also the general activation of the muscles.

*2.3. Similarity index*

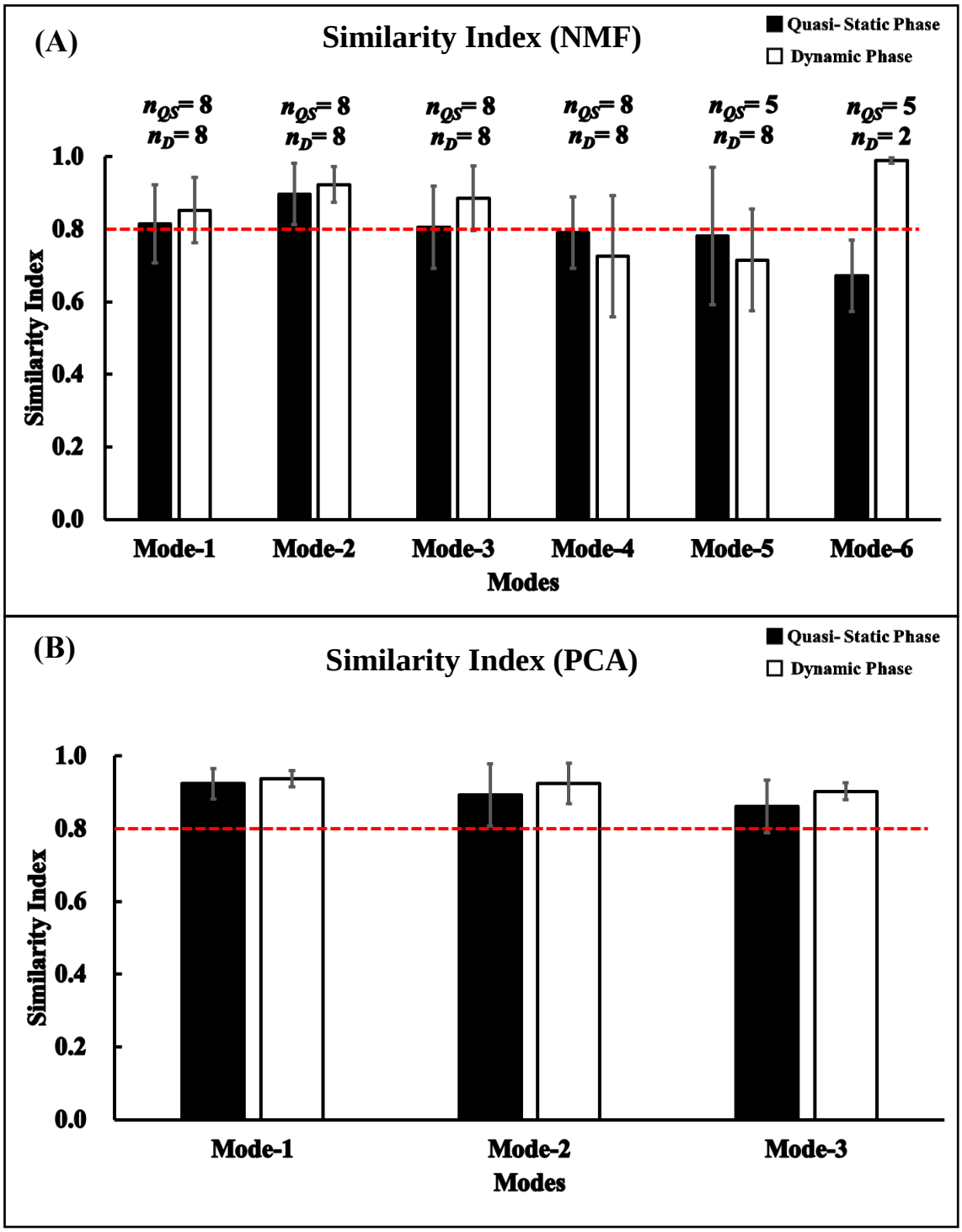


**Figure 7:** Average (±SE) similarity index across subjects for (A) NMF and (B) PCA.

*Significance value of similarity index > 0.8. $n_{QS}$ : number of subjects in a mode for quasi-static phase & $n_D$ : number of subjects in a mode for dynamic phase.

The similarity index was determined separately for PCA and NMF as mentioned in the methods. Figure 7 shows the average similarity index across subjects for M-modes extracted using PCA for both phases. Based on our criterion (*similarity index > 0.8*), all of the three M-modes were significantly similar for both phases. Figure- shows the average similarity index across subjects for M-modes extracted using NMF analysis for both phases. Note that due to dissimilarity in number of subjects after 4 modes for two phases, the number of subjects were indicated. Based on our criterion (*similarity index > 0.8*), first three M-modes were significantly similar for both phases. In case of modes 4 and 5 the values were between *0.7 and 0.8* on average across subjects for both phases with no significant difference between phases. Finally, for mode 6, average similarity index was *0.67 (±0.10)* across subjects for quasi-static phase whereas, in case of dynamic phase, similarity index was *0.98 (±0.01)* across subjects. The high similarity index in case of dynamic phase for mode 6 might be due to the reduced number of subjects, which is 2, and the activation coefficients of the muscles were similar.

### *2.4. Degrees of freedom (DOF)*

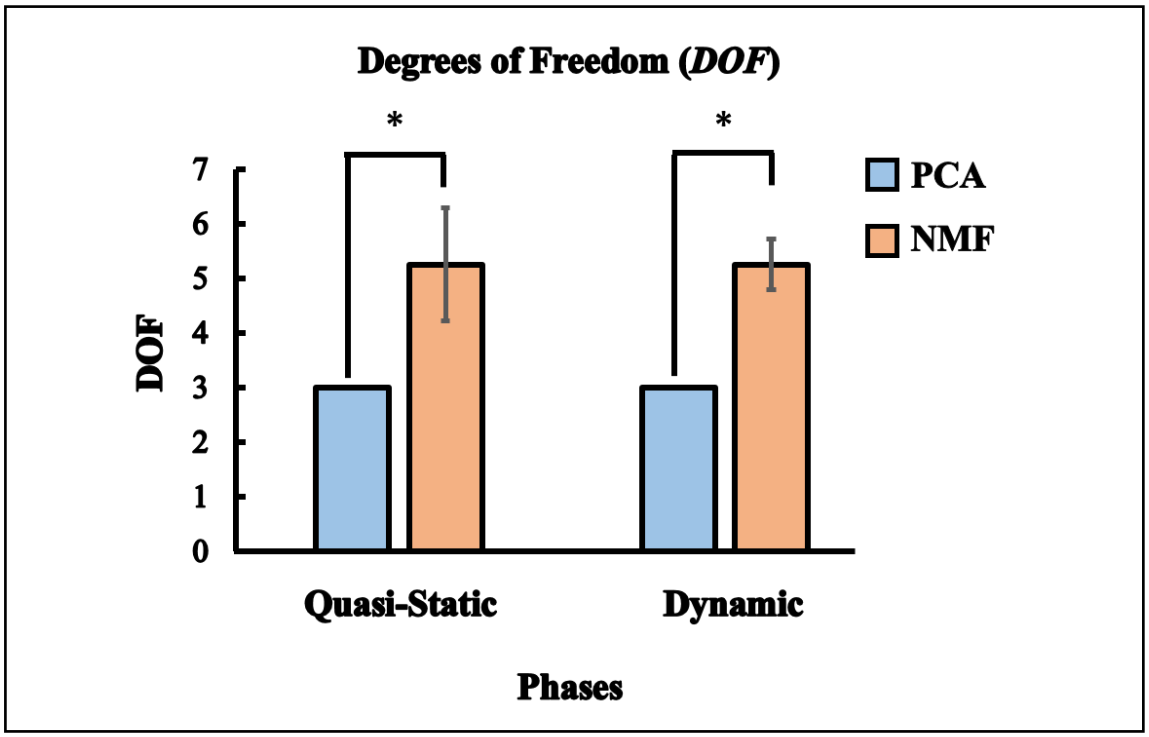


**Figure 8:** Average (±SE) (A) degrees of freedom (DOF) across subjects using NMF and PCA for both phases.

* indicates statistical significance.

As mentioned above in the results, average M-modes extracted using PCA and NMF was *3* and *5.25 ± 1.04* respectively for quasi-static phase, whereas, average extracted M-modes for dynamic phase was *3* and *5.25 ± 0.46* respectively (Figure 8). There was significant difference in degrees of freedom for NMF and PCA for quasi-static phase, $t(14) = 3.416$, $p < 0.05$ and dynamic phase, $t(14) = 7.638$, $p < 0.05$.

## 3. Synergy indices (ΔV)

The average synergy index throughout the phase was calculated for both phases. Average synergy indices across subjects was found to be positive ($\Delta V > 0$) in all directions (Figure 9). There was no statistical difference between the mean synergy index for both quasi-static and dynamic phases.

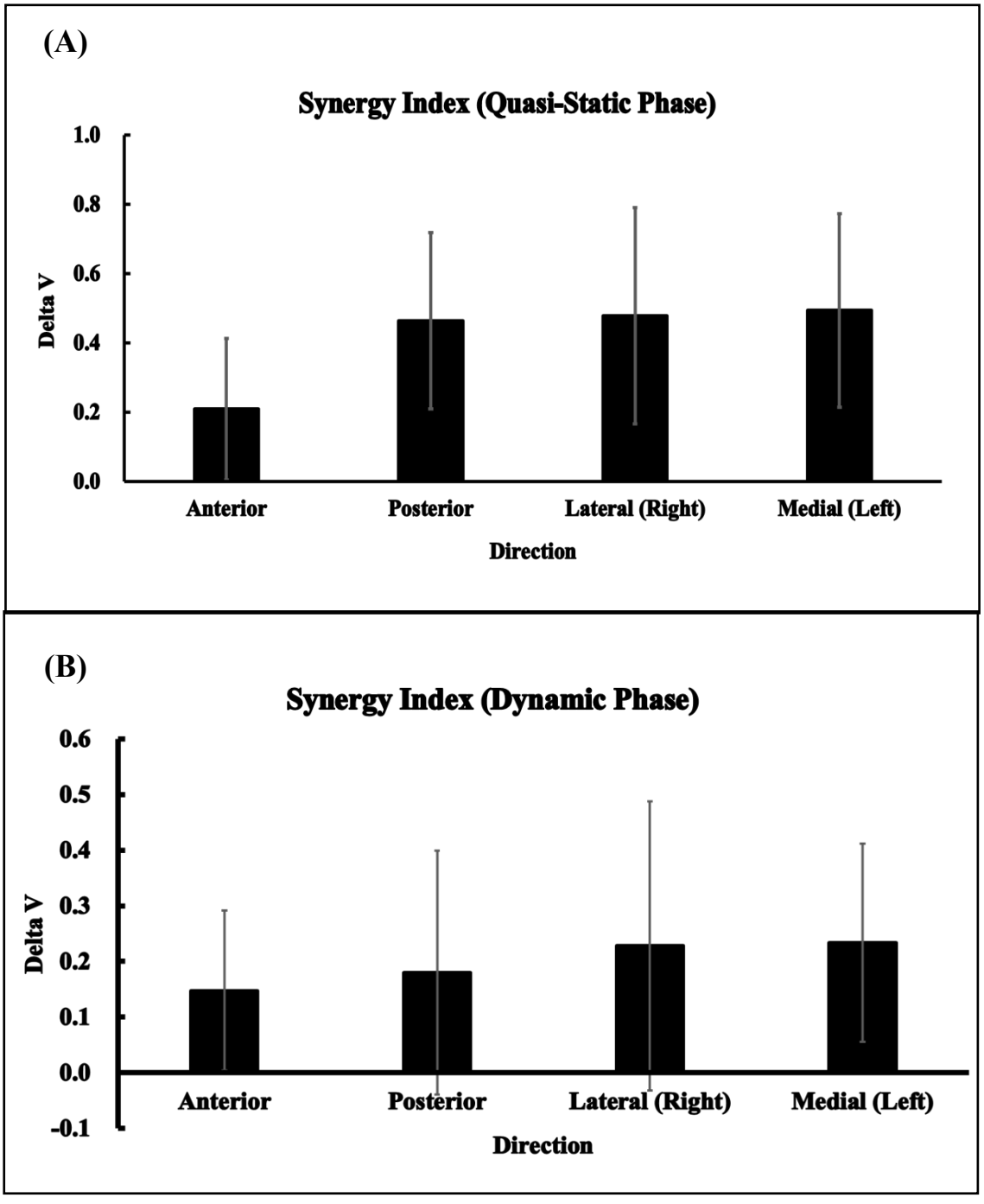


**Figure 9:** Average synergy index (±SE) across subjects for (A) Quasi-static and (B) Dynamic phase

# V. Discussion and Conclusion

The main goal of the study was to explore the difference in nature of M-modes extracted from different computational frameworks during multi-directional voluntary postural body sway task. The results support all three of our hypothesis. First, utilizing both computational frameworks, reduced degrees of freedom was observed i.e., mode control was done (*Hypothesis – I*). Secondly, the number of modes extracted using NMF was significantly larger than modes extracted using PCA (*Hypothesis – II*). Finally, for both phases average value of synergy indices across subjects was greater than 0 in all directions (*Hypothesis – III*) even though, no significant effect of direction was observed. Further, the results observed from the M-modes extracted using these two computational frameworks gives us further idea into the muscular control during postural sway which is discussed in following sections.

## 1. Differences in computational frameworks and its neurophysiological interpretation

The computational framework for both PCA and NMF is mainly concerned towards decreasing the initial muscular degrees of freedom into functional muscle groups (*M-modes*) defining the characteristics of a motor action (Danna-dos-Santos et al., 2007; Krishnamoorthy et al., 2003). The fundamental theory behind the dimension reduction is quite similar for both PCA and NMF with the exception of the constraint imposed in the algorithm. PCA & NMF imposes orthogonal and non-negative constraint respectively so based on these constraints, PCA allows for both negative and positive values (Wold et al., 1987) to the basis vectors whereas, NMF allows only positive values (Lee & Seung, 2001). In a physiological perspective, non-negative values aligns well with the activation property of muscles which is positive (Danion & Latash, 2011; Delis, Berret, Pozzo, & Panzeri, 2013). In case of having both positive and negative values, it might be advantageous if deviations from a certain baseline value of muscle activation is to be considered (Latash, 2012).

Additionally, the positive and negative values can be considered as excitatory and inhibitory effect on motor output respectively (Danion & Latash, 2011). In a multi-direction postural sway experiment concerned with this experiment, using PCA one might be able to observe the deviation of the muscle activations from the initial position (baseline) to change in activation on a certain direction. Then the muscles being activated from a baseline would have positive activation values whereas, muscles minimally activated or deactivated with progression of movement would have a negative activation values.

Further, the constraints associated with these computational frameworks might give us an idea on the nature of the basis vectors furthering our knowledge on the differences between the M-modes extracted using PCA and NMF. PCA imposes orthogonal constraint leading to non-overlapping basis vectors which complement each other to form a whole part (Sotiras, Resnick, & Davatzikos, 2015). In addition, the concept of 'orthogonal' allows maximization of the expressive power of the basis vector and avoids detrimental information not related to the task (Mailloux, Peck, Koster, & Van Wijngaarden, 1969). Unlike PCA or ICA which imposes orthogonal or independent constraint, NMF aims towards providing a sparse and part-wise representation of the elements to create a localized and disjoint groups of elements (Lee & Seung, 2001; Pascual-Montano, Carazo, Kochi, Lehmann, & Pascual-Marqui, 2006). However, NMF non-negative constraint does not allow restriction on the overlap of the basis vectors. Hence, this algorithm allows some undesirable overlapping of the basis vectors (Miettinen, Mielikäinen, Gionis, Das, & Mannila, 2008; Pascual-Montano et al., 2006). This has been observed in one of the experiments where they implemented NMF algorithm developed by Lee and Seung (algorithm used in our study) to facial database. It gave factor's images which was a part-based representation of the original images. There were high degree of undesirable overlaps between the parts particularly on the areas with common features of most of the images (Pascual-Montano et al., 2006). In context of our research, the overlap between the basis vectors can be interpreted as role of a single or a group of muscles participating in multiple neural pathways or processes leading towards postural control (Devarajan, 2008; Gaujoux & Seoighe, 2010). Based on this interpretation, PCA is most likely to determine the preference of a muscle or group of muscles

while, NMF is most likely to determine all the muscles or group of muscles following the neural pathways leading to postural control. In fact the extensive overlapping basis vectors was observed for the modes extracted using NMF whereas, the basis vector extracted using PCA had minimal to no overlap (Figure 6(A)). For example, looking at the activation level of the ES, we see that for NMF it is being significantly activated in mode-1 and mode-4 whereas, it is significantly activated in mode-3 for PCA. Similar activation levels were also observed for other muscles as well for both computational frameworks (Figure 5(A)).

Therefore proponents of each method might argue the viability of each of the methods while extracting modes based on the nature of their basis vectors and its neurophysiological interpretation. NMF with its non-negative constraint aligns well with the activation of the activation property of the muscles. Further one might also argue that muscles being multi-functional should ideally follow numerous neural pathways in order to accomplish postural control. In contrast PCA with its orthogonal constraint allows to determine the functional nature of the muscles to account for mechanical effect while controlling one's COP during postural control (Danna-dos-Santos et al., 2007; Furmanek et al., 2017; Krishnamoorthy et al., 2003). Hence, rather than deciding which method is superior, looking through the nature of cumulative modes and neurophysiological evidences we might be able to understand the originating level of these modes in context of neuro-motor hierarchy.

## 2. Neuro-motor hierarchy of M-modes extracted using PCA and NMF

Before postulating the neuro-motor hierarchy of the M-modes extracted using PCA and NMF, we must first understand the coordination of neural signals at different levels of neuro-motor hierarchy (cortical and subcortical). A prominent neurophysiologist James Huck (2005) developed a model of the information flow and coordination in CNS where firstly, cerebral cortical areas consists of substantial network of overlapped circuitry mainly associated with pattern formation (J. C. Houk, 2005). The information is looped into the sub-cortical areas namely, cerebellum and basal ganglia. Cerebellum functions for refinement and amplification of the neural signals mainly concerned with

reduction in error associated with a motor action. In case of basal ganglia, it functions as embodiment and classification of a coordinated pattern of neural signals. Hence, a pattern of neural signal is formulated at the cerebral cortex and when passed through the loop of subcortical components, the signal is refined through feedback information and further controlled by set of facilitator and inhibitors (spiny neurons & purkinje cells) to classify coordinated patterns (J. Houk, 1995; J. C. Houk, 2005; Merker, 2013). Additionally, the neural signal originating from vast cortical circuitry is converged using the principle of many-to-few such that subcortical structure has a compact flow of neural signals. Hence, flow of neural signals in cortical-subcortical system is designed so as to have a steep convergence ratio such that a clearer final estimate of the cortical signals at subcortical level would provide optimal estimate of behavior of motor action (Merker, 2013). In other words, there is a systematic decrease in degrees of freedom from cortical to subcortical level.

Now let us look at our results and postulate level of neuro-motor hierarchy based on the nature of the M-modes and components of CNS. Here the degrees of freedom extracted using NMF is significantly higher than using PCA for both phases (Figure 8). Based on the theory that there is a level-wise decrease in the degrees of freedom moving from cortical to effector level, M-modes extracted using NMF can be placed at a higher level than that using PCA. Further, we observed that the M-modes extracted using NMF had a higher degree of overlap than that for PCA which aligns well with the nature of the basis vectors mentioned in the previous section. Also, looking through the muscles activated for each mode for NMF numerous muscles were significantly activated for more than one mode while for PCA, specific groups of muscles were significantly activated for each mode across subjects (Figure 5(A) & 6(A)). These results are similar across subjects which was confirmed by the similarity index of each mode being either higher than or closer to significance level for both PCA and NMF (one exception was mode-6 extracted using NMF) (Figure 7). Hence, the components within the modes are overlapping over each other portraying a web-like nature across modes. This overlapping behavior seems to be similar to that of neural signals originating from the cortical level. There are few experiments were direct measurement of the nature of the neural signals from the primary motor cortex was performed. In one of these experiment, the neural signals originating from

the primates was measured for finger and wrist flexion & extension (Schieber & Hibbard, 1993). It was determined that for any given movement there was an initial firing of neurons not related to the task finger. It was followed by overlapping nature of neural activation in various intensity with large activation of neurons related to task and mild activation of neurons not related to the task (Schieber & Hibbard, 1993). This nature of initial firing of neurons was seen in first mode (broad activation) extracted using NMF. Additionally, the overlapping nature of the M-modes was also similar to the cortical level neural activation. Therefore, these evidences combined together we might argue that M-modes extracted using NMF might have cortical origin.

For PCA, as we mentioned above a functional interpretability of the muscles to account for mechanical effect while controlling one's COP during postural control can be determined. For a task associated with this study such as multi-directional postural sway, ideally the functional group of muscles to perform the task would be the muscle being activated to primarily control the motion in each direction. An anterior direction motion would be functionally controlled by activation of muscles in dorsal part of the body and vice versa for the posterior direction. This form of functional grouping of muscles was confirmed by the activation pattern and the modes formed in our study and similar other studies (Furmanek et al., 2017; Krishnamoorthy et al., 2003). This can be solidified with the results from our study as each mode extracted using PCA (Figure 6(A)). Also, the orthogonal constraint is an important condition for determination of synergy. Synergy itself has been assumed to be coordination originating at the sub-cortical level (J. C. Houk, 2005). There are many studies where the origination of synergies from sub-cortical level has been determined. In both postural control (Falaki, Huang, Lewis, & Latash, 2017) and multi-finger force production task (Park, Lewis, Huang, & Latash, 2014) for PD patients, the synergy index significantly improved after taking dopamine medication. It has been well documented that dopamine medication helps improve the coordination for PD patients. This increase in synergy indices extracted using PCA when on dopamine medication shows a direct effect on the coordination of movement. Therefore, M-modes extracted using PCA might be similar to coordination observed in the sub-cortical level. Further, the average synergy indices across subjects was positive for both phases, so the modes extracted using PCA coordinate to

stabilize one's posture. Hence, this coordinated behavior of M-modes extracted through PCA and average synergy indices being positive allows us to postulate the similarity between coordination observed in PCA with coordination of neural signals in sub-cortical level. Additionally, the negative values obtained in the components of M-modes are assumed to be inhibitory nature of the muscles. The function of the inhibitors (spiny neurons & purkinje cells) present in the sub-cortical structure seems to have similar property as the inhibition observed in PCA. Cumulatively these evidences lets us make an argument that the M-modes extracted using PCA might have a sub-cortical origin.

## 3. Future direction of research

As we have hypothesized the similarity in M-modes extracted using NMF and PCA are similar to neural signals originating from cortical and sub-cortical levels respectively. However, to concretely prove this hypothesis, a clinical study might be required with patients having cortical and sub-cortical impairment. Firstly, for studies involving stroke patients (with cortical impairment), it was determined for reaching task, the overall performance error (target reaching error) was significantly high but multi-joint synergy index was similar compared to age-matched healthy control (Reisman & Scholz, 2003). This shows that the even though impairments is observed in neural signals originating from the cortical level, the coordination at the sub-cortical level is sufficiently intact. In contrast for Parkinson patients (sub-cortical impairment), during multi-finger force production task, there were mild changes in overall performance with significant changes in synergy index compared to age-matched control subjects (Park, Lewis, Huang, & Latash, 2013; Park, Wu, Lewis, Huang, & Latash, 2012). Hence, to prove the hypothesis regarding the neuro-motor hierarchy of M-modes extracted using these two computational frameworks, firstly we need to perform postural sway task for age and gender matched stroke, PD and control subjects. If the hypothesis is to be true, the M-modes extracted using NMF and PCA would be similar to PD & Stroke patients respectively with dissimilarity in the reversed condition.

# References


Bernstein, N. (1947). On the construction of movements. *Medgiz, Moscow*.

Bernstein, N. (1966). The co-ordination and regulation of movements. *The co-ordination and regulation of movements*.

Bizzi, E., & Cheung, V. C. (2013). The neural origin of muscle synergies. *Frontiers in computational neuroscience, 7*, 51.

Bowden, B. S., & Bowden, J. M. (2014). *An illustrated atlas of the skeletal muscles*: Morton Publishing Company.

Cheung, V. C., Turolla, A., Agostini, M., Silvoni, S., Bennis, C., Kasi, P., . . . Bizzi, E. (2012). Muscle synergy patterns as physiological markers of motor cortical damage. *Proceedings of the National Academy of Sciences, 109*(36), 14652-14656.

d'Avella, A., & Tresch, M. C. (2002). *Modularity in the motor system: decomposition of muscle patterns as combinations of time-varying synergies.* Paper presented at the Advances in neural information processing systems.

Danion, F., & Latash, M. L. (2011). *Motor control: theories, experiments, and applications*: Oxford University Press.

Danna-dos-Santos, A., Slomka, K., Zatsiorsky, V. M., & Latash, M. L. (2007). Muscle modes and synergies during voluntary body sway. *Experimental brain research, 179*(4), 533-550.

Delis, I., Berret, B., Pozzo, T., & Panzeri, S. (2013). A methodology for assessing the effect of correlations among muscle synergy activations on task-discriminating information. *Frontiers in computational neuroscience, 7*, 54.

Devarajan, K. (2008). Nonnegative matrix factorization: an analytical and interpretive tool in computational biology. *PLoS computational biology, 4*(7), e1000029.

Falaki, A., Huang, X., Lewis, M. M., & Latash, M. L. (2017). Dopaminergic modulation of multi-muscle synergies in postural tasks performed by patients with Parkinson's disease. *Journal of Electromyography and Kinesiology, 33*, 20-26.

Ferdjallah, M., Harris, G. F., Smith, P., & Wertsch, J. J. (2002). Analysis of postural control synergies during quiet standing in healthy children and children with cerebral palsy. *Clinical Biomechanics, 17*(3), 203-210.

Furmanek, M. P., Solnik, S., Piscitelli, D., Rasouli, O., Falaki, A., & Latash, M. L. (2017). Synergies and Motor Equivalence in Voluntary Sway Tasks: The Effects of Visual and Mechanical Constraints. *Journal of motor behavior*, 1-18.

Gage, W. H., Winter, D. A., Frank, J. S., & Adkin, A. L. (2004). Kinematic and kinetic validity of the inverted pendulum model in quiet standing. *Gait & posture, 19*(2), 124-132.

Gaujoux, R., & Seoighe, C. (2010). A flexible R package for nonnegative matrix factorization. *BMC bioinformatics, 11*(1), 367.

Gelfand, I. M., & Latash, M. L. (1998). On the problem of adequate language in motor control. *Motor control, 2*(4), 306-313.

Houk, J. (1995). Information processing in modular circuits linking basal ganglia and cerebral cortex. *Models of information processing in the basal ganglia*, 3-9.

Houk, J. C. (2005). Agents of the mind. *Biological cybernetics, 92*(6), 427-437.

Jackson, J. H. (1889). On the comparative study of diseases of the nervous system. *Br Med J, 2*, 355-362.

Kaiser, H. F. (1962). Formulas for component scores. *Psychometrika, 27*(1), 83-87.

Krishnamoorthy, V., Latash, M. L., Scholz, J. P., & Zatsiorsky, V. M. (2003). Muscle synergies during shifts of the center of pressure by standing persons. *Experimental brain research, 152*(3), 281-292.

Kuo, A. D. (2007). The six determinants of gait and the inverted pendulum analogy: A dynamic walking perspective. *Human movement science, 26*(4), 617-656.

Kutch, J. J., Kuo, A. D., Bloch, A. M., & Rymer, W. Z. (2008). Endpoint force fluctuations reveal flexible rather than synergistic patterns of muscle cooperation. *Journal of neurophysiology, 100*(5), 2455-2471.

Lambert-Shirzad, N., & Van der Loos, H. M. (2016). On identifying kinematic and muscle synergies: a comparison of matrix factorization methods using experimental data from the healthy population. *Journal of neurophysiology, 117*(1), 290-302.

Latash, M. L. (2008). *Synergy*: Oxford University Press.

Latash, M. L. (2012). *Fundamentals of motor control*: Academic Press.

Latash, M. L., Scholz, J. P., & Schöner, G. (2002). Motor control strategies revealed in the structure of motor variability. *Exercise and sport sciences reviews, 30*(1), 26-31.

Latash, M. L., Scholz, J. P., & Schöner, G. (2007). Toward a new theory of motor synergies. *Motor control, 11*(3), 276-308.

Lee, D. D., & Seung, H. S. (1999). Learning the parts of objects by non-negative matrix factorization. *Nature, 401*(6755), 788-791.

Lee, D. D., & Seung, H. S. (2001). *Algorithms for non-negative matrix factorization.* Paper presented at the Advances in neural information processing systems.

Mailloux, B. J., Peck, J. E. L., Koster, C. H., & Van Wijngaarden, A. (1969). Report on the algorithmic language ALGOL 68 *Report on the algorithmic language ALGOL 68* (pp. 80-218): Springer.

Merker, B. H. (2013). The efference cascade, consciousness, and its self: Naturalizing the first person pivot of action control. *Frontiers in Psychology, 4*, 501.

Miettinen, P., Mielikäinen, T., Gionis, A., Das, G., & Mannila, H. (2008). The discrete basis problem. *IEEE Transactions on Knowledge and Data Engineering, 20*(10), 1348-1362.

Oba, N., Sasagawa, S., Yamamoto, A., & Nakazawa, K. (2015). Difference in postural control during quiet standing between young children and adults: assessment with center of mass acceleration. *PloS one, 10*(10), e0140235.

Palastanga, N., Field, D., & Soames, R. (2006). *Anatomy and human movement: structure and function* (Vol. 20056): Elsevier Health Sciences.

Park, J., Lewis, M. M., Huang, X., & Latash, M. L. (2013). Effects of olivo-ponto-cerebellar atrophy (OPCA) on finger interaction and coordination. *Clinical Neurophysiology, 124*(5), 991-998.

Park, J., Lewis, M. M., Huang, X., & Latash, M. L. (2014). Dopaminergic modulation of motor coordinaton in Parkinson's disease. *Parkinsonism & related disorders, 20*(1), 64-68.

Park, J., Wu, Y.-H., Lewis, M. M., Huang, X., & Latash, M. L. (2012). Changes in multifinger interaction and coordination in Parkinson's disease. *Journal of neurophysiology, 108*(3), 915-924.

Park, J., Zatsiorsky, V. M., & Latash, M. L. (2010). Optimality vs. variability: an example of multi-finger redundant tasks. *Experimental brain research, 207*(1-2), 119-132.

Pascual-Montano, A., Carazo, J. M., Kochi, K., Lehmann, D., & Pascual-Marqui, R. D. (2006). Nonsmooth nonnegative matrix factorization (nsNMF). *IEEE transactions on pattern analysis and machine intelligence, 28*(3), 403-415.

Reisman, D. S., & Scholz, J. P. (2003). Aspects of joint coordination are preserved during pointing in persons with post-stroke hemiparesis. *Brain, 126*(11), 2510-2527.

Roh, J., Rymer, W. Z., Perreault, E. J., Yoo, S. B., & Beer, R. F. (2013). Alterations in upper limb muscle synergy structure in chronic stroke survivors. *Journal of neurophysiology, 109*(3), 768-781.

Sabatini, A. M. (2002). Identification of neuromuscular synergies in natural upper-arm movements. *Biological cybernetics, 86*(4), 253-262.

Schieber, M. H., & Hibbard, L. S. (1993). How somatotopic is the motor cortex hand area? *Science, 261*(5120), 489-492.

Scholz, J. P., & Schöner, G. (1999). The uncontrolled manifold concept: identifying control variables for a functional task. *Experimental brain research, 126*(3), 289-306.

Sotiras, A., Resnick, S. M., & Davatzikos, C. (2015). Finding imaging patterns of structural covariance via non-negative matrix factorization. *NeuroImage, 108*, 1-16.

Tresch, M. C., Cheung, V. C., & d'Avella, A. (2006). Matrix factorization algorithms for the identification of muscle synergies: evaluation on simulated and experimental data sets. *Journal of neurophysiology, 95*(4), 2199-2212.

Wold, S., Esbensen, K., & Geladi, P. (1987). Principal component analysis. *Chemometrics and intelligent laboratory systems, 2*(1-3), 37-52.

Woollacott, M. H., Shumway-Cook, A., & Nashner, L. M. (1986). Aging and posture control: changes in sensory organization and muscular coordination. *The International Journal of Aging and Human Development, 23*(2), 97-114.

## 국문초록

# 다중 방향 자세 동요 과제 시 근육 모드 산출을 위한 Computational Framework

**파톡프라밧**

**체육교육학과**

**대학원**

**서울대학교**

본 연구의 목적은 근육 모드 (M-modes)를 결정하는데 사용되는 주성분분석(PCA)과 비 음수 행렬 인수분해(NMF)의 차이를 평가하는 것이다. PCA 는 각 성분의 직교성을 제약조건으로 가지며, NMF 는 비 음수 제약조건을 가진다. 이러한 차이로 인하여 두 방법 간 추출된 M-mode 의 생리적 특성에 따른 해석은 차이를 지닌다. 따라서 본 연구는 M-mode 의 산출의 차이를 확인하기 위하여 여러 방향 자세 기울이기 과제를 사용하였으며, 1) PCA 와 NMF 에 의해 자유도가 감소될 것이며, 2) PCA 방식에서 NMF 보다 더 큰 자유도의 감소가 나타날 것이며, 3) 모든 방향에서의 평균 시너지 지수는 0 보다 클 것이라는 가설을 가지고 진행 되었다.

연구 참여자로 선정된 건강한 성인 남녀 8 명은 발목 전략을 사용하여 전 후방, 좌우의 네 방향으로 최대 자발적 편차의 80% 수준까지 압력 중심(COP)을 이동시키는 과제를 총 15 회 수행 하였다. 자세기울이기 과제는 quasi-static 와 dynamic phases 의 두 단계로 구분하였으며, 몸통과 오른쪽 다리의 11 개 근육에서 근전도를 취득하였다. 적분근전도 값을 이용하여 자세 기울이기 과제의 두 단계에 대한 M-mode 가 PCA 와 NMF 에 의해 산출되었다. 또한, PCA 를 사용하여 추출된 M-modes 를 이용하여 각 방향에 대한 공동작용 지수와 두 단계에서의 시너지 지수를 산출하였다.

연구 결과, 전방으로의 COP 이동이 다른 방향들 보다 유의하게 높은 것으로 나타났으며($p < 0.05$), 발목에서의 움직임이 다른 관절에 비해 모든 방향에서 더 높은 변위를 갖는 것으로 나타났다. NMF 에 의한 M-modes 의 자유도는 quasi-static, dynamic phases 에서 각각 5.25±1.04, 5.25±0.46 으로 나타난 반면, PCA 에서는 두 단계 모두 3 으로 나타났다. 독립 t-검정 결과, 모든 단계에서 NMF 에 의해 산출된 M-modes 의 자유도가 PCA 보다 유의하게 높은 것으로 나타났다($p < 0.05$). NMF 와 PCA 분석을 통한 근육의 분류는 자세기울이기 과제 수행 시 특정 방향에 대한 설명력을 가지는 것으로 확인되었으며, 두 가지 방식으로 산출된 M-mode 는 유사성 지수를 바탕으로 두 단계 모두에서 피험자 간 유사함을 확인 하였다. 또한, 모든 단계에서 평균 공동작용지수는 0 보다 큰 것으로 나타났으며, 방향에 따른 유의한 차이는 나타나지 않아 사전에 설정한 연구 가설을 모두 검증할 수 있었다.

본 연구는 NMF 과 PCA 를 사용하여 추출된 M-modes 간 차이를 확인하는 한편, 이를 운동제어 계층(피질 및 피질 하부)의 여러 수준에의 신경 활동 특성으로 설명 하고자 하였다. NMF 의 비 음수 제약조건은 M-mode 의 각 요소들이 양의 값을 가짐을 의미하며 이는 근육 활성화의 특성과 일치된다. 반면, PCA 의 제약조건인 mode 간 직교성은 특정 기저에 대해 근육 활성이 양 또는 음의 값으로 나타남을 의미한다. 또한 NMF 에 의해 산출된 기저 벡터의 정사영(projection)은 높은 확률로 중첩되며 이는 대뇌 피질에서의 신경

활동과 유사한 특징을 가진다. 반면, PCA 에서 기저 벡터의 정사영은 낮은 확률로 중첩 되며, 이는 피질하부의 신경 활동과 유사한 특성을 지닌다. PCA 에 의해 산출된 공동작용 지수는 피질하부 수준에서 일어나는 신경 활동에 의한 것이라고 알려져 있으며, 따라서 PCA 를 사용해 추출한 M-mode 또한 피질하부에서 일어나는 신경 활동을 반영할 수 있다. 그러나 NMF 와 PCA 를 통해 추출한 M-mode 의 신경학적 위계는 추가적인 임상 실험을 통해 규명되어야 할 것이다.

**주요어:** 근육 모드 (M-modes), 주성분분석 (PCA), 비음수 행렬 인수분해 (NMF), 다중 방향 자세 동요, 자유도 (DOF), 공동작용, 신경 모터 계급

**학번:** 2016 - 23105